Student thesis series INES nr 358

Modelling vegetation dynamics and carbon fluxes in a high Arctic mire

Laura Reinelt

2015

Department of

Physical Geography and Ecosystems Science

Lund University

Sölvegatan 12

S-223 62 Lund

Laura Reinelt (2015). Modelling vegetation dynamics and carbon fluxes in a high Arctic mire.

Master degree thesis, 30 credits in *Physical Geography and Ecosystem Analysis*

Department of Physical Geography and Ecosystems Science, Lund University

Level: Master of Science (MSc)

Course duration: *September* 2014 until *January* 2015

Disclaimer

Modelling vegetation dynamics and carbon fluxes in a high Arctic mire

---

Laura Reinelt

Master thesis, 30 credits, in *Physical Geography and Ecosystem Analysis*

Supervisors:

Paul Miller

Department of Physical Geography and Ecosystem Science

Lena Ström

Department of Physical Geography and Ecosystem Science

Exam committee:

Marko Scholze

Department of Physical Geography and Ecosystem Science

Dan Metcalfe

Department of Physical Geography and Ecosystem Science

Abstract

High Arctic wetlands are an important component of the global climate system. Nevertheless estimations of their expected response to climate change and associated climate-feedbacks have large uncertainties. Improving models for vegetation and carbon dynamics of ecosystems is an important step towards making predictions more accurate. In this study, an arctic-enabled version of the LPJ-GUESS dynamic global vegetation model (LPJ-GUESS-WHyMe) was used to conduct a local modelling study on vegetation dynamics and carbon fluxes in the high Arctic mire Rylekærene in north-western Greenland. LPJ-GUESS-WHyMe includes process descriptions of wetland hydrology, soil freezing and wetland carbon (carbon dioxide and methane) emission, as well as wetland PFTs. The aims of this study were: 1) to assess uncertainties of parameters and process representations; 2) to assess the possibility of including grazing into the model; and 3) to lay a ground for future studies in which the response of the mire ecosystem to climate change and changes in grazing pressure can be simulated. Field data from several studies in Rylekærene were used for parameter calibration and comparison with model outputs. The field data includes carbon dioxide and methane flux chamber measurements, measurements of environmental variables and vegetation analyses. Model parameters were calibrated in the following order: 1) hydrology and permafrost; 2) vegetation; and 3) methane dynamics, using data from 2013. Data from 2011 was used for validation. The calibration improved model performance within hydrology, permafrost and vegetation dynamics for both 2013 and 2011. For methane fluxes the calibration did not improve the model performance for 2011. Sensitivity analyses were performed for parameters related to vegetation and methane dynamics. An important finding in the sensitivity study was that increasing the fraction of vascular plant net primary production allocated to root exudates also decreased vascular plant productivity which had a net-effect of decreasing methane emissions. Main challenges for future studies were identified to be: 1) the inclusion of the effect of run-on/off from snowmelt on soil hydrology and temperature; 2) modeling competition between grasses and mosses; and 3) modeling the effect of graminoid density on methane fluxes accurately. Data from a three-year musk-ox exclosure experiment was used to build a simple module for modelling changes in grazing pressure. The results showed that improvements in the representation of model processes are needed to represent the effects of musk ox grazing on different parts of the ecosystem accurately.

Key words: Geography, Physical Geography, LPJ-GUESS, Ecosystem modelling, Vegetation dynamics, Biogeochemical cycling, Methane dynamics, High Arctic wetland, Zackenberg

Table of contents

1. Introduction

1.1 Importance of the Arctic and Arctic wetlands for the climate system

The Arctic is an important part of the global climate system. The high albedo of snow and ice makes the region important for the global radiation balance, the cold temperatures play an important role in global atmospheric and oceanic circulation patterns and the arctic carbon cycle is a key component of the global carbon cycle, to name only some aspects (ACIA 2005). Understanding how the arctic is changing, how it will change as a response to global climate change and how these changes will result in feedback mechanisms that will either enhance or mitigate global warming is thus crucial for predicting global climate change and its consequences (McGuire et al. 2006).

1.1.1 Arctic amplification

What makes the need to understand arctic climate feedbacks even more pressing is the fact that the global warming trend in mean air surface temperature is more pronounced in high northern latitudes than in other parts of the globe (Serreze and Barry 2011). In the last 30 years, temperatures have risen 0.6 °C per decade in high northern latitudes, which is twice as fast as the global average (IPCC 2013). This arctic amplification of climate change is caused by several factors such as lowered albedo due to reduced sea ice extent and soot on snow, changes in cloud cover and increased concentrations of black carbon aerosol (Serreze and Barry 2011). Arctic amplification is expected to become even stronger in the future (IPCC 2013).

1.1.2 The arctic tundra biome

At present, the arctic tundra biome covers about 8% of the global land surface (McGuire et al. 2012). It is mostly underlain by continuous permafrost and the vegetation consists of vascular plants, mosses, lichens, shrubs and dwarf shrubs. Trees are almost entirely absent (McGuire et al. 2012). The carbon cycle of the arctic tundra biome is both highly complex and sensitive to changing conditions (McGuire et al. 2009). Its response to climate change is a key feedback mechanism that will most likely enhance the global warming trend, but it is uncertain by how much (McGuire et al. 2009). This is firstly because currently there are gaps in the understanding of the arctic tundra carbon cycle and its expected response to climate change. Secondly, much of the existing knowledge has not been incorporated into process-based ecosystem models (McGuire et al. 2009; McGuire et al. 2012; Wullschleger et al. 2014; Schuur et al. 2015). Until recently, scientists concluded from the available data on arctic carbon fluxes and pools that arctic tundra has been a sink of carbon dioxide (CO_2) on an annual basis for the last 10 000 years and that it may become a source as a result of climate change (Pries et al. 2012). A recent study by Belshe et al. (2013) however suggested that arctic tundra has been a source of CO_2 to the atmosphere since the 1980s. To understand the interactions between the arctic tundra carbon cycle and global climate it is also necessary to take into account fluxes of methane (CH_4) (IPCC 2013). The amount of carbon exchanged between ecosystems and atmosphere in form of CH_4 is small compared

to the fluxes of CO_2, but CH_4 is a much more potent greenhouse gas, having a global warming potential 34 times as high as that of CO_2 over a 100-year time horizon (IPCC 2013).

1.1.3 Arctic wetlands

Arctic wetlands are an especially important part of the arctic tundra carbon cycle as the cold and wet conditions lead to slow decomposition and the build-up of large carbon pools in peat layers (Tarnocai et al. 2009). As precipitation is very low in the arctic region and occurs mostly during the winter in form of snow (ACIA 2005), wetlands are distributed in patches that can be found in areas where the hydrogeomorphological conditions allow water from snow melt, streams, lakes or the sea to inundate the area (Woo and Young 2003). Estimations of the present total carbon content of northern peatlands range between 200 and 450 Pg of carbon (McGuire et al. 2009). In comparison, the atmospheric carbon pool currently amounts to 828 Pg of carbon (IPCC 2013). Also, wetlands are sources of CH_4 to the atmosphere due to inundated and in turn anoxic soil conditions.

1.1.4 Carbon cycling in arctic wetlands

Figure 1 shows the most important pools and fluxes of the carbon cycle in a high arctic peatland and some of the processes and factors controlling their magnitudes, as described in Schlesinger and Bernhardt (2013). Plants convert light energy from photosynthetically active radiation (PAR, 400-700nm wavelength) into chemical energy in form of carbohydrates through the process of photosynthesis. The general equation of photosynthesis is

$$CO_2 + H_2O + light\ energy \longrightarrow CH_2O + O_2$$

The water used in the process is mostly taken up from the soil through plant roots (Schlesinger and Bernhardt 2013). CO_2 and O_2 are exchanged with the atmosphere through pores on the epidermis of plant tissues, called stomata. Also H_2O is lost through to the atmosphere through the stomata (transpiration). Plants open and close their stomata depending on air humidity and atmospheric CO_2 concentration to maximize carbon uptake and minimize water loss (Farquhar and Sharkey 1982). The amount of carbon fixed by photosynthesis depends on green plant biomass, plant species, PAR, water availability, air humidity, temperature and atmospheric CO_2-concentration. About half of the CO_2 taken up through photosynthesis is released back into the atmosphere through autotrophic respiration, which can be divided into growth- and maintenance respiration. In this process energy from carbohydrates is used for plant growth and maintenance. The rest of the carbohydrates are stored in the form of plant tissues and transferred into other carbon pools after some period of time: some plant parts are grazed by herbivores and some die or are emitted as root exudates and become part of the litter and soil pools. Some become affected by disturbance such as fire, so that carbon is re-emitted into the atmosphere. Herbivores use a part of the carbon compounds they consume for respiration, a part for building their body and a part is defecated. Carbon compounds from all of these pools are broken down by decomposing macro- and microorganisms, in the presence of O_2 through aerobic decomposition, during which carbon is released into the atmosphere as CO_2. The rate and pathway of

decomposition depends on many factors such as temperature, water availability (which is determined by precipitation, hydrology and permafrost dynamics), the quality and quantity of carbon compounds and the community of heterotrophic organisms. (Schlesinger and Bernhardt 2013)

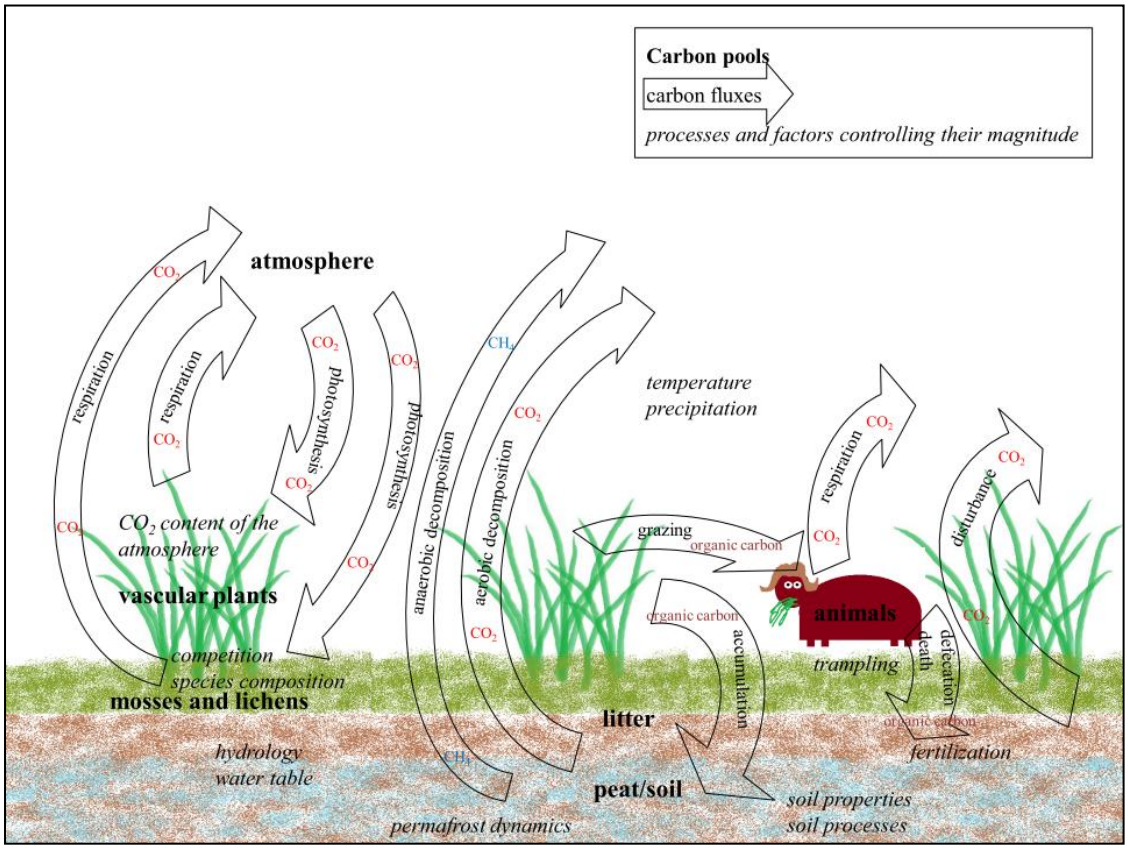

Figure 1: The most important pools and fluxes of the carbon cycle in a high arctic peatland and some of the processes and factors controlling their magnitudes.

On an ecosystem scale, the fluxes of CO_2 between an ecosystem and the atmosphere are described by the following terms:

- GPP (gross primary production) is the CO_2 taken up by plants through photosynthesis
- R_a (autotrophic respiration) is the CO_2 emitted by plants through respiration
- NPP (net primary production) is GPP - R_a
- R_h (heterotrophic respiration) is the CO_2 emitted by decomposing organisms
- R_{eco} (ecosystem respiration) is $R_a + R_h$
- NEP (net ecosystem production) is GPP - R_{eco}
- NEE (net ecosystem exchange) is a measurement of the net CO_2 flux between an ecosystem and the atmosphere

1.1.5 Methane dynamics in arctic wetlands

The production and oxidation of CH_4, its pathways of emission and the most important controls on their magnitudes are shown in Figure 2. Methane is produced during anaerobic decomposition, which

is a complex process with several steps and pathways carried out by different species of anaerobic microorganisms, including methanogenic archae (Stams and Plugge 2010). Anaerobic decomposition is significantly slower than aerobic decomposition (Schlesinger and Bernhardt 2013). Under waterlogged, anaerobic conditions carbon compounds can be reduced through alternative processes under the use of an alternative electron acceptor other than O_2. From most to least energetically favourable these processes are NO^{3-}, Mn^{4+}, Fe^{3+} and SO_4^{2-} reduction and methanogenesis (Schlesinger and Bernhardt 2013). Methanogenesis is the most common pathway in wetlands, even though it is the least energetically favourable, as the availability of the other electron acceptors is often limited (Schlesinger and Bernhardt 2013). Methanogens can use hydrogen and CO_2 formate, carbon monoxide, methanol, methylated compounds or acetate as substrates for methanogenesis and finally emit both CH_4 and CO_2 (Stams and Plugge 2010). Thus, for the decomposition of most carbon compounds methanogenesis is preceded by a number of microbial fermentation processes that generate substrates for methanogenesis, which is often a limiting factor for methanogenesis (Schlesinger and Bernhardt 2013). Root exudates of vascular plants have been shown to be important for substrate availability as they have increase the concentration of acetic acid in the root vicinity which can be used by methanogens (Ström et al. 2012). The amount of root exudates differs between vascular plant species and has been shown to be particularly high in *Eriophorum scheuchzeri* (Ström et al. 2012)

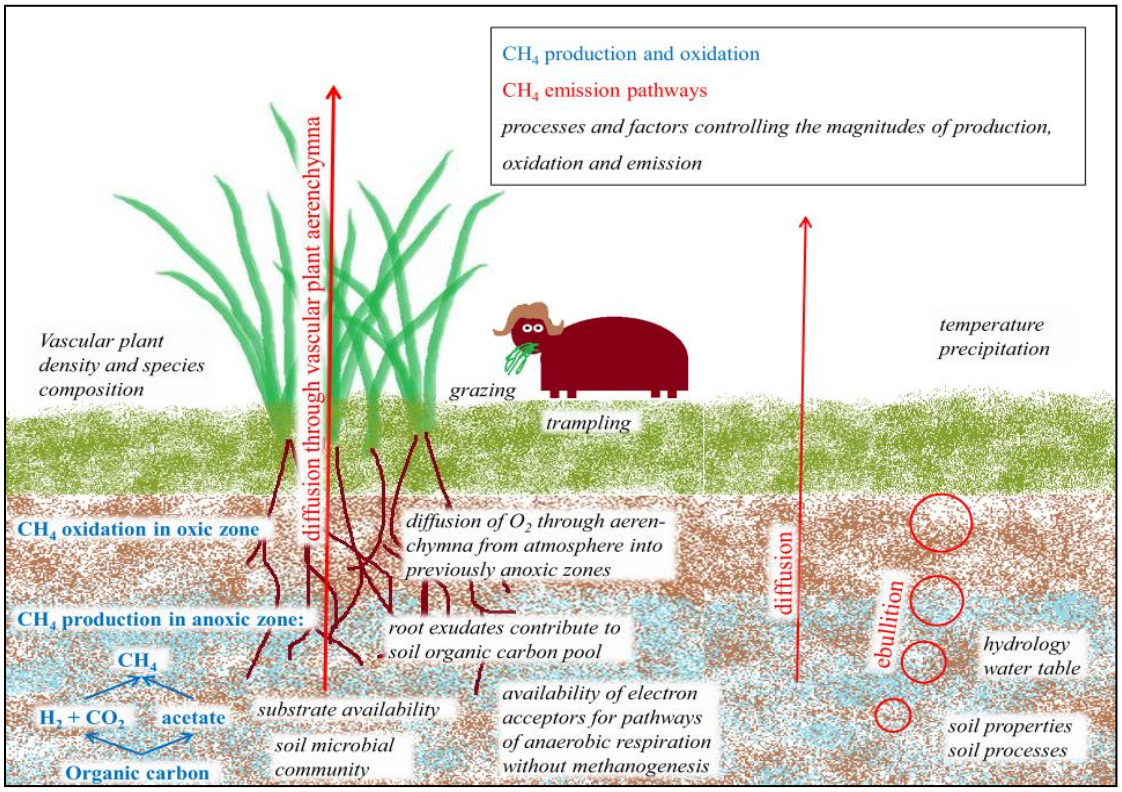

Figure 2: The production and oxidation of CH_4, its pathways of emission and the most important controls on their magnitudes.

A fraction of the produced CH_4 is oxidized by methanotrophic bacteria in oxic zones of the soil before it can reach the atmosphere (Schlesinger and Bernhardt 2013). Oxic zones are found above the water table and close to the roots of vascular plants, as wetland vascular plants have airspaces within their cortex (aerenchymna) that transport O_2 the roots as an adaptation to the inundated conditions (Schlesinger and Bernhardt 2013).

There are three pathways through which CH_4 is emitted to the atmosphere: diffusion, ebullition and mediation through aerenchyma of vascular plants, which not only mediate O_2 from the atmosphere to the roots, but also CH4 from the roots to the atmosphere (Schlesinger and Bernhardt 2013). A significant part of the CH_4 that diffuses through the soil is oxidized before reaching the atmosphere, while through the two other pathways the CH_4 passes through the oxic layer more quickly, so that less CH_4 is oxidized (Schlesinger and Bernhardt 2013).

CH_4 emissions in wetlands show high variability at small and large temporal and spatial scales, due to the many processes involved, which makes it hard to make estimations of global emissions (Schlesinger and Bernhardt 2013). Olefeldt et al. (2013) found that large parts of the variation in average growing season fluxes of CH_4 between 303 sites in permafrost regions could be related to water table position, soil temperature and vascular plant cover. Also the species composition of the vascular plant cover and substrate availability have been shown to be significant, especially the presence of *Eriophorum sp* (Ström et al. 2015). Seasonal variations have been found to be strongly related to date of snow melt, soil temperature and water table position (Mastepanov et al. 2013).

1.1.6 Arctic wetlands and climate change

Climate change is likely to change both arctic wetland extent and carbon cycling within arctic wetlands (McGuire et al. 2009). Modelling studies project a temperature increase in the Arctic of 2.8 ºC to 4.6 ºC by 2071–2090 compared to 1981-2000 and precipitation increase of 7.5 to 18.1% (ACIA 2005). Precipitation increase is predicted to occur mostly in autumn and winter and to have a high spatial variability, reaching up to 35% in some areas (ACIA, 2005). Permafrost thawing is a crucial process for future wetland extent, but it is currently not possible to predict whether wetland extent is going to increase or decrease as a result, since the thawing can happen in two different ways with possibly opposing outcomes: a continuous top-down thawing of the surface layer makes the soil drier and reduces wetland extent, while abrupt thawing with thermokarst leads to the formation of more wetlands and lakes in some areas and drying in others (Schuur et al. 2015). Permafrost thawing makes available more carbon for decomposing microorganisms and also both aerobic and anaerobic decomposition occur faster under warmer conditions (Schuur et al. 2015). Decomposition in wetlands is slower, so wetland formation may slow down the release of carbon into the atmosphere, while wetland degradation accelerates it (Schuur et al. 2015). However, especially high CH_4 emissions have been measured in thermokarst wetlands (Olefeldt et al. 2013). Drying of peatlands combined with warmer temperatures may also lead to wildfires with high sudden carbon emissions (Mack et al.

2011). Increased soil carbon emissions may be partially offset by increased photosynthesis, driven by higher temperatures, longer growing seasons, higher CO_2 content of the atmosphere and a higher nutrient availability due to increased decomposition (Schuur et al. 2015). Such a greening of arctic ecosystems has already been observed (Xu et al. 2013). Also, climate warming has been shown to lead to shrub-expansion into areas that were previously graminoid dominated which leads to an increased CO_2 uptake (Myers-Smith et al. 2011).

1.1.7 Arctic wetlands and herbivory

An important factor to consider in many wetlands is herbivory by large mammals such as caribous, reindeers and musk-oxen (Stark and Ylänne 2015). Herbivores affect many of the processes of the wetland carbon cycle either directly or indirectly through grazing, trampling and defecation, so changing densities of herbivores may alter ecosystem properties including the carbon balance significantly (Stark and Ylänne 2015). On the other hand, herbivore densities are dependent on environmental conditions such as forage availability and climate, so that climate change may have large impacts on herbivore densities (Berg et al. 2008).

There have been a number of studies on impacts of herbivores on arctic wetland ecosystems, which have recently been reviewed by Stark and Ylänne (2015). Many studies have reported similar influences of herbivores on vegetation composition: higher grazing pressure favored graminoids and herbs, while lower grazing pressure favored mosses (Cahoon et al. 2012; Olofsson et al. 2009; Falk et al. 2015) and, if climatic conditions allow it, shrubs (e.g. Post and Pedersen et al. 2008; Olofsson et al. 2009). This could be explained by the slower growth of mosses and shrubs that make them more sensitive to trampling than graminoids and herbs, which can re-grow quickly. Falk et al. (2015) also found changes in graminoid species composition. Also, herbivory has been found to decrease litter biomass (Sjogersten et al. 2011; Falk et al. 2015). In a study by Olofsson et al. (2004) changes in soil temperature were measured, that can be linked to the insulating function of moss- and litter layers which keep the soil from warming. Higher soil temperatures may lead to permafrost thawing and lower soil moistures, all of which enhances soil decomposition.

There have also been a number of studies on the impact of herbivores on the carbon balance of arctic ecosystems, with differing results. Most studies found no change in NPP or a decrease with increased grazing pressure (e.g. Sjogersten et al. 2011; Cahoon et al. 2009), while some found an increase in NPP (e. g. Olofsson et al. 2004; Falk et al. 2015). Fewer studies have addressed the impact of grazing on CH_4 fluxes: Sjogersten et al. (2011) and Sjoegersten et al. (2012) found no changes in CH_4 fluxes. Falk et al. (2015) found increased CH_4 emissions in grazed plots. These findings point towards that the net effect of grazing on the carbon balance can be different depending on ecosystems and herbivore type and densities.

1.2 Modelling arctic wetland vegetation dynamics and biogeochemistry

1.2.1 Purposes of process-based ecosystem modelling

Ecosystem modelling has been a fast-evolving area of research, especially over the last 20 years. Process-based ecosystem models can be used to address a variety of questions by combining and extrapolating knowledge that has been gained from different branches of ecosystem research. Modelling the response of ecosystems to changing climate and their feedbacks to the global climate system is currently one of the most predominant aims of ecosystem modelling research (Scheiter et al. 2013). Predicting global climate change is important for decisions of policymakers on regulations of greenhouse gas emissions, land use etc. and also for mitigation measures. Climate predictions are being made with the help of earth system models that simulate the processes within and interactions between atmosphere, ocean and land through a system of equations, algorithms and parameterizations (IPCC 2013). Modelling land surface processes is a crucial part of this and especially models of terrestrial vegetation and its role in the global carbon cycle is still a source of major uncertainty within earth system models (IPCC 2013). In order to be included into a coupled land-ocean-atmosphere earth system model that can simulate climate change accurately, the land surface model needs to include both vegetation dynamics across time and space according to changes in climate and atmospheric CO_2 concentration and biogeochemical fluxes through the ecosystems (Haxeltine and Prentice 1996). A study by Cox et al. (2000) was the first time that a dynamic global vegetation model with biogeochemical cycling was included into an earth system model and since then more models have been developed with more processes and refined process representations.

Apart from being used within earth system models, models of biogeochemistry and vegetation dynamics can be used to address a range of further scientific questions, for example: How will a specific ecosystem respond to changing environmental conditions, to land use change or to disturbance? They can also be used to quantify processes that are difficult to measure by applying and combining known principles.

1.2.2 Strategies for ecosystem model development

The improvement of models that simulate the processes and components of complex natural systems is a cyclical process of model development, parameter calibration, validation using measurement data, sensitivity analysis, revisiting the model development to improve critical processes, initiating more measurements, and so on (Smith and Smith 2007). For assessing and improving dynamic vegetation models, it is important to conduct studies not only on a global scale, but also at smaller scales like regions, catchments or a specific site (Pappas et al. 2015). Modelling studies of smaller scales that include the comparison of modeled properties to field observations allow the evaluation of processes in much more detail than large-scale studies, as much more detailed field data can be used for comparison in local studies. Also, small-scale studies take less computing power, so that extensive sensitivity studies and calibration procedures can be performed more easily. To validate the model's

ability to reproduce regional and global pools, fluxes and vegetation distributions however, regional and global studies are necessary, in which model results are compared to, for example, inventory databases, inverse modelling estimates and maps of the distribution of vegetation (Sitch et al. 2003).

"All models are wrong, some are useful" (Box and Draper 1987) is a famous saying by the statistician George Box that is referred to often in the context of ecosystem modelling. All model outputs have uncertainty and it is important to quantify the uncertainty in order to draw valid conclusions from modelling studies. Uncertainty of model outputs can be either due to inaccurate implementation of the processes involved (conceptual uncertainty) or due to uncertainty in the parameterization (parameter uncertainty). For model development this means that the detail in which processes are represented needs to be chosen carefully: processes should be represented as accurately as possible, as long as there is enough data available to either set the parameters directly, or to calibrate them. Additionally, limitations in computing power need to be taken into account. (Smith and Smith 2007)

1.2.3 Challenges of modelling arctic wetland carbon dynamics

Modelling arctic tundra (and particularly arctic tundra wetland) vegetation and carbon dynamics poses many challenges. Some of them are similar to the challenges in other biomes and some are specific to the arctic. One is the representation of vegetation. Most dynamic vegetation models group vegetation into plant functional types (PFTs). Each PFT is characterized by a set of trait parameters specifying its role in ecosystem functioning and the environmental conditions under which it can establish and grow. A recent review on the representation of vegetation in dynamic vegetation models in high-latitude ecosystems pointed out the following problems (Wullschleger et al. 2014):

- PFTs are currently too general to accurately represent above- and belowground traits of vegetation over a range of different species and ecosystems
- Especially root traits and the partitioning of biomass between above- and belowground are represented in a simplistic way. Roots in arctic ecosystem have been shown to be very important for ecosystem functioning and to differ substantially between species
- Mosses and lichens are missing in many models (or represented in too simply in others), even though they play an important role in ecosystem functioning and show great functional differences between species (Turetsky et al. 2012). Mosses also significantly affect soil thermal and hydrological properties, by acting as an insulating layer and by decreasing evapotranspiration (Frolking et al. 2010).
- Models oversimplify competition between PFTs and individuals, disturbance and succession
- Almost no models include grazing, even though it has been shown to have very significant impacts on ecosystems and their vegetation (see section above)

There have been many studies addressing these issues and making improvements, but still much work is needed. Wullschleger et al. (2014) proposed the following approaches for future studies:

- Increase the diversity of PFT traits across ecosystems in model. This could be done for example through the use of trait-databases that include measured data on plant traits for different species and locations. Such a database was started in 2007 under the name TRY (Kattge et al. 2011) and has since been growing, but it still lacks information on many species and traits. Another possible approach would be a flexible implementation of plant trait parameters, for example through measured co-variations between traits and environmental conditions (Verheijen et al. 2013) or through the use of theories of community ecology (Scheiter et al. 2013).
- Implement or improve mechanisms that are currently missing or too simplified, like competition, disturbance, grazing, effects off moss on soil properties, etc.
- Conduct local and regional studies to choose appropriate PFTs, parameterizations and process implementations

Nutrient availability is a limiting factor in arctic ecosystems (Jonasson et al. 1999). Advances have been made to include nitrogen dynamics into dynamic vegetation modelling (Smith et al. 2014), but this has so far not been included in wetland models (Wania et al. 2013).

As CH_4 plays an important role for the climate system and since wetlands contribute substantially to CH_4 emissions (see section 1.1.5), a number of wetland models have been built that include methane dynamics. However, a recent model inter-comparison study between wetland methane models (Melton et al. 2013; Wania et al. 2013) led to the conclusion that there is currently still substantial parameter uncertainty as well as conceptual uncertainty regarding the processes of CH_4 production and emission in large-scale wetland models. To improve this, both studies on the driving factors of CH_4 emissions as well as more datasets for model validation and parameterization are needed (Melton et al. 2013).

Another challenge specific to wetland modelling is the estimation of both current and future wetland extent. Melton et al. (2013) Found very large differences in present wetland extent between the ten wetland CH_4 models they used within their model inter-comparison study. This led to a substantial addition of uncertainty in CH_4 emission. The differences were mainly due to the fact that some models used remotely sensed wetland fractional maps, while others estimated wetland extent based on prognostic simulations. For future studies it is thus important to model wetland extent accurately. Run-on and –off is an important factor for hydrology in many wetlands, especially in the arctic region (see above), so one approach is to couple a topographic model of runoff (as developed by Tang et al. (2014a), Tang et al. (2014b)) to a wetland/CH_4 model. Modelling permafrost dynamics is a related challenge. Even though advances have been made, presently none of the present permafrost models includes abrupt thawing, which is likely to be a very important process for wetland formation and extent (Schuur et al. 2015)

1.3 Aims

This thesis is a local modelling study of vegetation dynamics and carbon fluxes (CO_2 and CH_4) in a high arctic mire located in Zackenberg valley in north-eastern Greenland, where data on various ecosystem and environmental properties and processes have been collected. The model used in this study is an arctic-enabled version of the LPJ-GUESS (Smith et al. 2001; Smith et al. 2014) dynamic global vegetation model. This model version, hereafter referred to as LPJ-GUESS-WHyMe, includes process descriptions of wetland hydrology, soil freezing and wetland carbon (CO_2 and CH_4) emission, as well as wetland PFTs (Wania et al. 2009a, b, 2010; McGuire et al. 2012; Miller and Smith 2012; Zhang et al. 2013). The study is aimed at addressing some of the issues mentioned above regarding the improvement models of high latitude ecosystems. An additional aim is to lay a ground for performing future studies that simulate the response of the mire ecosystem to scenarios of climate change and changes in grazing pressure.

In detail, these aims will be addressed through the following steps:

1. Adapt LPJ- GUESS-WHyMe to the mire studied with its specific climate, soil conditions, hydrology and vegetation, based on a range of measurement data taken at the site in 2013.
2. Evaluate the model's performance using measurement data from 2011.
3. Compare the performance of the adapted model to the performance of the model with LPJ-GUESS-WHyMe standard parameters.
4. Test the model's sensitivity to different parameters to evaluate which processes need more accurate representation and for which parameters more accurate measurements are needed.
5. Test the model's ability to reproduce the effects of a 3-year musk-ox exclosure experiment that was conducted in the mire. This part of the study is a first step towards implementing a grazing module into LPJ-GUESS-WHyMe, which could simulate different scenarios of future grazing pressure (together with climate change).

2. Method and Data

2.1 Site description

The study site is the high arctic mire Rylekærene which is located in Zackenberg valley, close to Zackenberg Research Station in North Eastern Greenland (74°28′N, 20°31′W, see Figure 3). Various biotic and abiotic aspects of the ecosystems and influencing factors in Zackenberg valley have been monitored within the program Zackenberg Basic since it was started in 1996 (www.zackenberg.dk). The valley is underlain by continuous permafrost with active layer depth ranging between 45 and 80 cm (Christiansen et al. 2008). The annual mean temperature is around -9 °C. During winter, the area is mostly snow-covered and during polar night (89 days) mean monthly air temperatures are below -20 °C (Hansen et al. 2008). The average annual accumulated precipitation for the years 1996 to 2005 was 261 mm water equivalent. Summers are dry, with only 10% of the precipitation falling as rain. Snow melt usually begins in late May and ends in mid-June. July is the warmest month with a mean temperature of 5.8 °C. During the warmest 4 to 6 weeks in summer temperatures rarely drop below 0 °C (Hansen et al. 2008). The growing season starts with the end of snowmelt, typically in late May and lasts approximately 2 to 3 months, until the soil freezes again (Mastepanov et al. 2013). The five main plant communities that can be found in the valley are *Cassiope* heath, *Dyras* heath, grassland, mire and *Salix* snowbed, distributed depending on topography, soil properties and hydrology (Elberling et al. 2008).

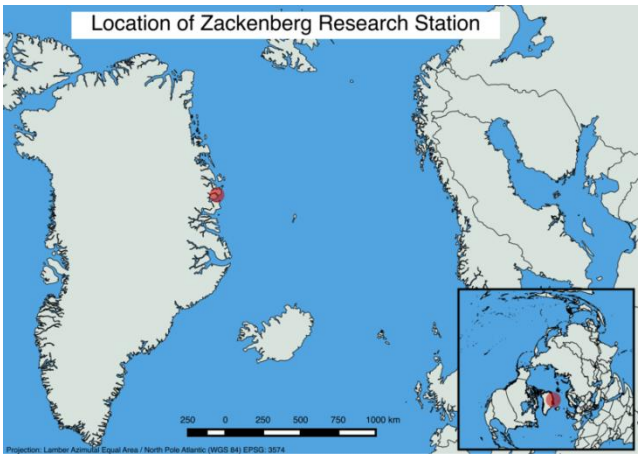

Figure 3: Map showing the location of Zackenberg Research Station.

Rylekærene is located in the lowland part of the valley at a flat slope. The peat layer in the mire is about 7 to 20 cm deep (Falk et al. 2015). The ground is covered by a dense moss layer (mainly *Tomenthypnum*, *Scorpidium*, *Aulacomnium* and *Drepanoclaudus*) (Ström et al. 2012) with vascular plants emerging through it, such as the sedges *Eriophorum scheuchzeri*, *Dupontia fisheri ssp. psilosantha*, *Carex sp.*, *Equisetum s.* and the grass *Arctagrostis latifolia*. The density and species composition of the vascular plants is patchy. Melt water flowing from the surrounding mountains into the valley and through the mire plays an important role for the hydrology and for the permafrost dynamics, raising the water table and adding energy during springtime and summer. Over the summer, the melt water flow decreases, so that the water table sinks and conditions get drier.

In summer, musk-oxen (*Ovibos moschatus*) range the valley in loose herds of varying size and frequently graze in the wetland. They are the only large herbivores in the area (Berg et al. 2008) and their summer diet has been found to consist of 80% graminoids (which can be found mainly in the mire) and 20% *Salix* (Kristensen et al. 2011). In winter they feed on vegetation, which they can reach through the snow. The musk-ox population in the valley has been monitored since 1996 within the Zackenberg BioBasis program (Forchhammer et al. 2008). Analysis of the population numbers from 1996 to 2005 showed a clear increase and also a strong dependence on winter snow conditions (Forchhammer et al. 2008). Higher snow cover went along with lower population number, due to difficulties reaching forage through the snow because of either too thick or too hard snow layers (Forchhammer et al. 2008). The future of the musk-ox population is uncertain. Climate warming may favor musk-ox populations through later snow in autumn, but on the other hand, thawing days during winter may cause ice layers to form in the snow that prevent musk-oxen from reaching the vegetation (Berg et al. 2008).

Changes in climate and vegetation composition in Zackenberg valley between 1997 to 2008 have been analyzed in a study by Schmidt et al. (2012). They found a significant increase in summer temperatures of between 1.8 and 2.7 °C per decade and also a decrease in spring snow cover and July, though not significant. The response of the vegetation differed between plant communities, but in all of them a significant decrease in cover of grasses and lichens and an increase in litter were found. In Rylekærene they found a significant decline in grasses (a reduction by almost 60% of the dominant grass species *Dupontia psilosantha*) a significant increase in mosses and litter and a small increase in shrubs, which they attributed mainly to drier conditions because of higher temperatures and a deepening active layer. The authors suspected that without the presence of grazing musk-oxen a stronger shrub expansion might have happened.

2.2 Data

The site-specific data for Rylekærene used in this study was partly obtained from long-term monitoring programs and partly collected within a number of studies and experiments that were conducted in the mire.

2.2.1 Climate data

The climate data (daily mean air temperature, daily precipitation and radiation) used for the years from 1995 to 2013 was measured at a meteorological station that has been in place since Zackenberg Research Station was founded in 1995. Since 1979 there is data available from a meteorological station at Daneborg, which is located 23 km south-southeast of Zackenberg Research station. This data was used for the years 1979 to 1994. Data of monthly mean temperature, monthly precipitation and cloud fraction for 1901 to 1978 and atmospheric CO_2 concentration for the entire period was provided by the Climatic Research Unit time-series datasets CRU TS 3.10 (Harris et al. 2014). This dataset holds global data for grid cells of 0.5° × 0.5° derived from averages and interpolation from

meteorological stations across the world's land areas and can be used to run the modal globally (Harris et al. 2014). Here data for the coordinates 74.5°N, 20.5°W was used. To drive LPJ-GUESS-WHyMe, quasi-daily values were derived from the monthly averages. To take into account the fact that the microclimate in the mire might be different from the gridcell average of the CRU dataset, the CRU data for temperature and precipitation of the years 1979 to 2011 was plotted against the monthly averages from the Zackenberg measurements and a linear regression was performed. For temperature, a linear relationship was found and the CRU data was adjusted accordingly for the years 1901 to 1979 (see section 3.1).

2.2.2 Exclosure experiment

Most of the field data used, including CO_2 and CH_4 fluxes, vegetation properties and environmental variables was collected within an experiment designed to study the effect of musk-ox grazing on the mire ecosystem in Rylekærene. A detailed description of the experiment can be found in Falk et al. (2015). For this experiment, five blocks of exclosure plots with controls were installed in the mire in 2010. Each of the blocks consists of three plots close to each other: an exclosure, a control and a snow control. Each exclosure subplot consists of a 10x10 m large area, which is fenced in by a one meter high sheep fence to keep the musk-oxen from entering. In control plots the corners were marked by 15-20 cm high steel poles, but no fence installed. In the snow control plots, fence was installed only on one side of the area, towards north-northwest, which is the dominant winter wind direction, to account for potential effect of the fences on snow dynamics. Only data from exclosures and control plots (not snow controls) was used in this study as the results of Falk et al.'s analysis pointed towards no effects of the fences on snow dynamics, but a tendency of the musk-oxen to graze less close to the snow fences.

In 2011 and 2013, vegetation analyses were conducted. In 2011 the vegetation analysis included only the tiller density of major vascular plant species in three of the blocks. In 2013, samples of biomass were taken from an area of 0.04 m² in each of the plots, dried and sorted into moss, vascular plant species and litter. For these samples, the number of tillers of major vascular species was counted and the number of green leaves of *Carex*, *Dupontia* and *Eriophorum* was counted.

In each of the years 2011 to 2013, CH_4 fluxes, NEE and R_e were measured throughout the major part of the growing season using a closed chamber technique, with a manual transparent plexiglas chamber (that was covered for dark measurements of R_e) and a gas analyzer. At the same time, water table position (wtp), active layer depth (ald) and soil temperature at 10 cm depth were monitored. Measurements were taken continuously throughout the period, covering 1 to 2 blocks a day on most days, measuring through all of the five blocks and starting over again once all of the blocks had been measured. Like this, approximately weekly measurements are available for each of the plots, in total six rounds of all blocks in 2013. For the analysis of this study, an average of the measurement results of each round was calculated and assigned to the average measuring day of that round together with a

standard deviation. For 2011, only data from block 3 was available, for five dates throughout the growing season.

GPP was calculated by subtracting R_{eco} (dark chamber flux) from NEE (transparent chamber flux). GPP was converted to daily averages that can be compared with the modeled daily averages by multiplying with 16 to account for changing insolation throughout the day. R_{eco} was assumed to remain constant throughout the day and NEE_{daily} was approximated as follows:

$$NEE_{daily} = 16 * NEE_{measured} + 8 * R_{eco}$$

In 2011 and 2012, no major differences could be measured between exclosure and control plots, but in 2013 significant changes in some properties were found. Table 1 shows the significant differences and similarities of a comparison between properties exclosures and control plots in 2013 compared to 2010, as determined through statistical analysis by Falk et al. (2015). The observed changes in wtd, ald and soil temperature are probably due to the fact that these properties were measured from the top of the moss layer, which was thicker inside the exclosures (Falk et al. 2015), so they were not considered in this study.

No significant difference in total vascular plant biomass or *Eriophorum scheuchzeri* biomass could be found in 2013, even though there was a significant difference in GPP and tiller density. However, not only green biomass was measured and according to Lena Ström (personal communication), it could be seen in the field that within the exclosures larger parts of the vascular plant biomass were not green than in the control plots. This is why we used the data on tiller density to approximate the loss in green biomass in the exclosures compared to control plots.

Table 1: Results from the muskox exclosure experiment (Falk et al. 2015)

Property	**Average value in control plots 2011 (±standard error)**	**Average value control plots 2013 (±standard error)**	**Average value exclosure plots 2013 (±standard error)**	**Significant differences between control and exclosure plots in 2013**
Total vascular plant tiller density (tillers/m²)	6136 (±555)	3845 (±375)	2180 (±325)	- 43 %
Eriophorum Scheuchzeri tiller density(tillers/m²)	2700 (±452)	1965 (±575)	915 (±175)	-53 %
Eriophorum Scheuchzeri fraction of total tillers	44 %	51 %	41 %	-10 %
Dry weight of litter biomass (kgC/m²)*	-	0.025 (±0.004)	0.081 (±0.017)	+ 224 %
Dry weight of moss biomass (kgC/m²)*	-	0.190 (±0.018)	0.295 (±0.020)	+ 55 %
Dry weight of vascular plant biomass (kgC/m²)*	-	0.087 (±0.026)	0.097 (±0.028)	not significant
Dry weight of *Eriophorum Scheuchzeri* biomass (kgC/m²)*	-	0.027 (±0.005)	0.030 (±0.006)	not significant
Density of vascular plant green leaves (leaves/m²)	-	5838 (±643)	2705 (±316)	- 54%
Density of *Eriophorum Scheuchzeri* green leaves (leaves/m²)	-	2743 (±697)	1240 (±278)	- 55 %
Average height of vascular plant tillers (cm)	-	10.9 (±0.7)	15.4 (±0.9)	+ 41 %
Average height of *Eriophorum Scheuchzeri* tillers (cm)	-	10.6 (±0.6)	14.6 (±0.9)	+ 34 %
NEE (mg CO_2/m²/h)	-338	-234	-124	- 47 %
Ecosystem respiration (mg CO_2/m²/h)	331	285	363	not significant
GPP (mg CO_2/m²/h)	667	-620	-487	- 21 %
CH_4 emission (mg CH_4/m²/h)	3	3	1.7	- 44 %
Water table depth (cm)	6.4	14.1	16.8	+ 19 %
Active layer depth (cm)	56.7	49.1	44.8	- 9 %
Soil temperature (°C)	7.7	5.2	4.6	- 12 %

*unit conversion from kg dried biomass/m² (as measured in the field) to kgC/m² (as simulated by the model) was done by multiplying a factor 0.44 (see section 2.2.3)

2.2.3 Data from additional measurements

Estimation of fraction of NPP allocated to root exudates

In the LPJ-GUESS-WHyMe, root exudates are quantified by allocating a fraction f_{exu} of NPP to a root exudates pool (see section 2.3.3). An approximation for this parameter was deduced from data collected in two studies in Rylekærene.

The first study, described in Ström et al. (2003), was designed to investigate how species-specific root exudation patterns affect the availability of acetate and CH_4-emissions. In a laboratory experiment with monoliths collected in the mire it was found that *Eriophorum scheuchzeri* emitted root exudates of 14.3 mgC/m^2/h and *Dupontia psilosantha* emitted root exudates of 4.0 mgC m^{-2} h^{-1}. However, CO_2 fluxes and biomass of the monoliths were not measured in this study, so we estimated it using data from a second study. In this study, described in Ström and Christensen (2007), it was investigated how plots with dominance of *Eriophorum scheuchzeri* plots with dominance of other sedges (*Carex stans* and *Dupontia psilosantha*) differed in below-ground concentrations of low molecular weight carbon compounds and CO_2 and CH_4 fluxes. Table two shows the results for mean seasonal GPP and green leaf biomass of Eriophorum scheuchzeri and total vascular plants in the plots with low/high *Eriophorum scheuchzeri* density.

Table 2: Mean seasonal GPP and green leaf biomass of *Eriophorum scheuchzeri* and total vascular plants as measured in Ström and Christensen (2007).

	Low *Eriophorum scheuchzeri*	High *Eriophorum scheuchzeri*
mean seasonal GPP (mgC/m²/h)	235 (±15)	315 (±44)
Eriophorum scheuchzeri dried green leaf biomass (kgC/m^2)*	0.0038 (±0.0007)	0.0225 (±0.0054)
total vascular plant dried green leaf biomass (kgC/m²)*	0.0283 (±0.0025)	0.0404 (±0.0100)

*unit conversion from kg dried biomass/m² (as measured in the field) to kgC/m² (as simulated by the model) was done by multiplying a factor 0.44 (see section 2.2.3)

NPP is approximately half of GPP (Schlesinger and Bernhardt 2013), so we estimated NPP in these plots as GPP/2. We assumed that the NPP in the high *Eriophorum scheuchzeri* plot was similar to NPP of the *Eriophorum scheuchzeri* monoliths and NPP in the low *Eriophorum scheuchzeri* plots similar to NPP of the *Dupontia psilosantha* monoliths. Using this we estimated that *Eriophorum scheuchzeri* allocates 9.0% of NPP to root exudates and other vascular plant species allocate 3.4% of NPP to root exudates. As in the control plots in 2013 51% of the tillers were *Eriophorum scheuchzeri* tillers, we set f_{exu}=6.2% in the model. For simulating exclosure we set f_{exu}=5.4% as 41% of the tillers inside the exclosures were *Eriophorum scheuchzeri* tillers.

GPP of moss-only plots

Falk et al. (2014) made an experiment to study the effect of simulated increased grazing on carbon allocation patterns in Rylekærene. Within this study CO_2 fluxes were measured in plots where all

vascular plants were removed, so that the vegetation in these plots consisted only of mosses. They found that GPP in plots without vascular plants was 11% of the GPP in control plots. This information was used for calibration of vegetation parameters (see section 2.4).

N and C content of biomass

Biomass within the model is quantified in the unit kgC/m², while the field biomass data has the unit kg of dried biomass/m². Also some of the relationships within the model that include biomass are originally formulated for the unit kg of dried biomass/m². Measurements of C and N content of vascular plant biomass (Ström, unpublished results) lead to the following unit conversion:

$$mass\ [kgC/m^2] = mass[kg/m^2] * \ 0.44$$

2.3 Model description

LPJ-GUESS-WHyMe is a process-based wetland dynamics and carbon emission model that includes vegetation dynamics (McGuire et al. 2012; Zhang et al. 2013; Tang et al. 2014b). It is an arctic-enabled version of LPJ-GUESS (Lund-Potsdam-Jena General Ecosystem Simulator) (Smith et al. 2001; Sitch et al. 2003; Gerten et al. 2004), which is a process-based dynamic vegetation model that includes biogeochemical cycling and can be applied from local to global scales. For the WHyMe (Wetland Hydrology and Methane) version, additional features important to wetland ecosystems were incorporated: permafrost dynamics, peatland hydrology, peatland PFTs and methane dynamics. These features were initially developed for LPJ-WHyMe, as described in (Wania et al. 2009a, b, 2010) and incorporated similarly into LPJ-GUESS-WHyMe. LPJ-DGVM (Lund-Potsdam-Jena Dynamic Global Vegetation Model) and LPJ-GUESS share the formulations of physiological and biogeochemical processes and use the same range of PFTs. The difference is, that LPJ-GUESS, which was initially intended especially for local and regional studies, explicitly simulates growth and competition among individual plants, while LPJ simulates average plant properties and interactions (Smith et al. 2001).

Figure 4 shows a schematic overview of the main properties and mechanisms modeled in LPJ-GUESS, with an overview the additions made for LPJ-GUESS-WHyMe. Each day, the modeled ecosystem state is characterized by a number of state variables, such as carbon pools (soil organic matter, vegetation and litter), vegetation structure and composition, water table position, soil temperature profile and NPP. Carbon is transferred between these pools and between the pools and the atmosphere through various processes. Some of them are modeled daily, such as peat soil hydrology, photosynthesis, plant respiration, plant phenology, soil microbial decomposition, CH_4 production, oxidation and transport and soil thermal processes such as heat diffusion, freezing and thawing. Other processes occur yearly, such as biomass allocation and growth, plant reproduction, establishment and mortality, fire disturbance (excluded in this study) and leaf and root turnover. The model can be run for a user-defined number of gridcells of size 0.5° × 0.5° with no interactions between the gridcells.

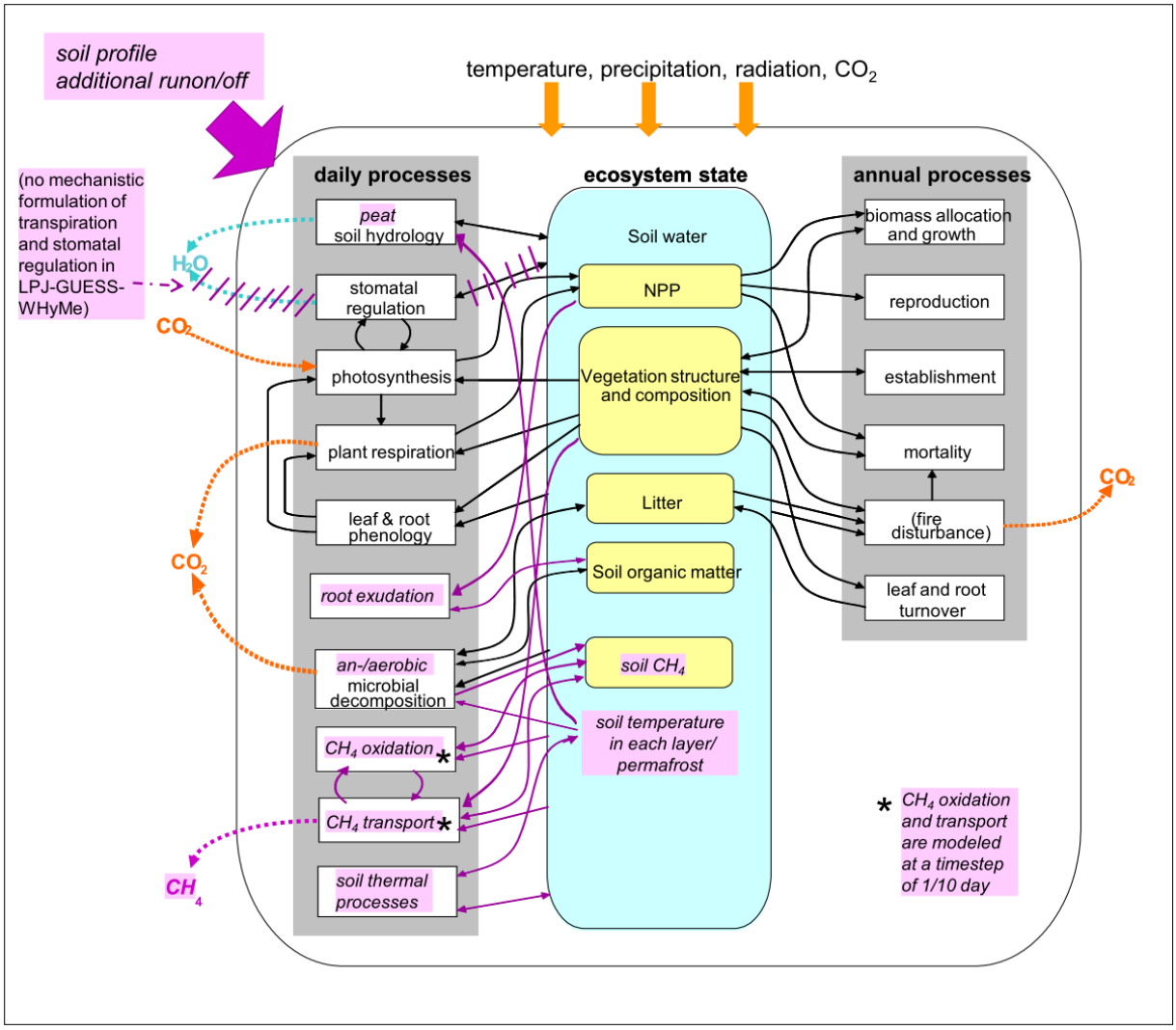

Figure 4: Conceptual diagram showing the main state variables, processes, gas fluxes between ecosystem and atmosphere and input data of LPJ-GUESS and LPJ-GUESS-WHyMe (WHyMe additions in purple).

In this study, the model was run for only one gridcell with the coordinates 74.5°N, 20.5°W. For a historical period of 1901 to 2013, the model was run with the climate data as described above (see section "Climate data"). Prior to the historical period, the model was run for a spin-up period of 500 years, during which the climate data from 1901 to 1930 was repeated. Atmospheric CO_2 concentration was held constant at the level of 1901 for the spin-up period (296 ppm). The collected data and knowledge about processes in Rylekærene were used to adapt GUESS-WHyMe to represent site-specific carbon pools and processes as accurately as possible. The changes made for adapting the model to the site are of four types: 1) Using site specific forcing data for climate and the soil profile, 2) Using site-specific values for some parameters for which measurements are available from the site or for which there were literature values from other arctic sites, 3) Calibration of parameters that have not been measured using data on fluxes and biomass measured in 2013, 4) Addition of site-specific processes in an empirical way. In the following sections, a detailed description of the relevant processes is given, including the changes that were made for adapting the model to the site. In section 2.3.4, a summary of all the changes is presented.

2.3.1 Soil characteristics and processes

In the standard-version of LPJ-GUESS-WHyMe, the soil column consists of four layers: a snow layer of variable thickness, a litter layer of 5cm (contrary to LPJ-GUESS, the litter layer in LPJ-GUESS-WHyMe has a fixed thickness as it is assumed that litter is quickly incorporated into the peat soil), a peat layer of 2m that is divided into sub-layers of 0.1 m, and a "padding" layer of depth 48 m with thicker sub-layers that serves to facilitate the calculation of soil temperatures. As the peat layer of the Rylekærene is only 7 to 20 cm thick the soil type in the lower 1.7 m of the peat layer was changed to mineral soil. The peat layer was not set lower than 30 cm because that would have complicated the hydrology scheme (see following section).

Peatland hydrology

The peat layer is divided into a 0.3 m acrotelm, within which the water table position can fluctuate, and a 1.7 m thick catotelm that is permanently saturated with water. Water table position is updated daily in response to precipitation, snowmelt, evapotranspiration, active layer depth and surface run-on/off. For this study, a daily additional external run-on/off was added to account for melt water coming from the mountains and flowing through the mire (see section 2.4). The calculation of evapotranspiration in the peatland hydrology scheme differs substantially from the non-peatland scheme in LPJ-GUESS. In non-peatland LPJ-GUESS, water that exceeds the soil's water holding capacity is assumed to disappear from the gridcell via subsurface-runoff, so that the soil can never be inundated. Evapotranspiration is simulated explicitly, including transpiration (depending on plant stomatal conduction for different PFTs), bare soil evaporation and interception loss (Gerten et al. 2004), depending on soil moisture, atmospheric demand, root structure and depth, leaf area and air temperature. In LPJ-GUESS-WHyMe, evapotranspiration is modeled using an empirical relationship depending on the water table position, with the addition of interception loss (which in the case of Rylekærene is low due to low summer precipitation). In LPJ-GUESS-WHyMe, transpiration consequently does not depend on photosynthesis.

Soil temperature and permafrost

The non-peatland version of LPJ-GUESS does not include a full vertical soil temperature profile. In LPJ-GUESS-WHyMe, temperatures for each layer of the soil column are updated daily by numerically solving the heat diffusion equation. Forcing consists of snow depth and daily air temperatures as well as on thermal diffusivity (which depends on the water content) of each soil layer. The model includes release and uptake of latent heat during thawing and freezing. The modeled active layer depth consists of the depth of the layers that have temperatures above 0 °C. Soil temperatures in the mire are strongly affected by melt water that brings additional energy into the mire (see section 2.1) and makes the soil thaw more quickly than in the surrounding non-inundated areas. This effect is not included in the implementation of external run-on/off in the model, so we chose to approximate this effect by multiplying a factor h_{runon} (see calibration procedure) to the latent heat that is released when soil water thaws. Even though the thawing of soil water and the inflow of melt water are not directly

related, we estimated that they would occur during the same time of the year as they are both driven by air temperatures.

2.3.2 Vegetation

PFTs

Model vegetation is grouped into a number of plant functional types (PFTs), each of which is characterized by a number of parameters. In this study, only two PFTs were used: wetland graminoids and mosses. The representation of graminoids and mosses is somewhat simpler than the representation of tree- and shrub-PFTs: for graminoids and mosses only one average individual is simulated, while for other PFTs several individuals of several age classes are simulated. The following description is restricted to modeled mechanisms for graminoids and grasses.

State of vegetation

The state of the vegetation of each PFT in each time step is characterized by leaf and root carbon mass (only leaf carbon mass for mosses) and foliar projective cover (fpc), which is the fraction of the gridcell that is covered by the PFT.

fpc, LAI, leaf carbon mass and leaf longevity

The relationship between fpc and leaf area index (LAI) is as follows, according to the Lambert-Beer law (Monsi and Saeki 1953):

$$fpc = 1.0 - \exp(-0.5 * LAI)$$

with

$$LAI = leaf\ carbon\ mass * SLA$$

where SLA is specific leaf area, which is calculated from leaf longevity a according to an empirical relationship by Reich et al. (1997):

$$SLA = 0.2 * \exp(6.15 - 0.46 * \log(a * 12.0)$$

For grasses, leaf longevity is one year. For mosses previously the same leaf longevity was assumed, but in this study we calibrated SLA_{moss} directly to account for the fact that mosses have non-photosynthetic tissue, which has previously not been taken into account.

NPP and plant growth

Carbon mass is updated at the end of each year by allocating the PFT's accumulated NPP obtained through daily photosynthesis throughout the year (minus a fraction allocated to reproduction) to roots and leaves. The model also contains formulations for annual mortality, establishment and leaf and root turnover.

Daily NPP is calculated as the balance of photosynthesis and autotrophic respiration. The absorbed photosynthetically active radiation ($APAR$) is calculated as follows:

$$APAR = PAR * f_{PAR} * \alpha_a$$

where f_{PAR} is a function of the PFT's LAI, phenology and the total LAI in the gridcell using Beer's law, that accounts for light competition.

φ is daily phenology and ranges between 0 and 1 (see section "phenology" below).

α_a is a scaling factor that was created to account for reduction in quantum efficiency from leaf to canopy level, but also accounts for missing mechanisms of nutrient limitation and scattering (Smith et al. 2014). It was calibrated to make modeled global carbon fluxes and pools agree with published estimates (Haxeltine and Prentice 1996). We considered in this study to recalibrate α_a separately for graminoids and mosses ($\alpha_{a,graminoid}$ and $\alpha_{a,moss}$) as arctic nutrient limitations differ from global nutrient limitation and as the parameter could compensate for the fact that mosses have non-photosynthetic tissue, which has previously not been taken into account. The recalibration however did not lead to results of biomass comparable to field observations, so we chose not to recalibrate these parameters.

Daily photosynthesis is calculated based on an adapted Farquhar scheme (Farquhar et al. 1980) and it depends on APAR, air temperature and the CO_2 concentration of the intercellular spaces in the leaf, with the assumption of no N-limitation. The CO_2 concentration of the intercellular spaces in the leaf mesophyll depends on atmospheric CO_2 concentration and on stomatal conductance, which in the non-peatland version of LPJ-GUESS depends on the balance between water demand and availability. In LPJ-GUESS-WHyMe it is assumed that the stomata are always open since water stress is not modeled explicitly (see section 2.3.1). The temperature dependence of photosynthesis differs between PFTs. Daily NPP is finally multiplied by a factor $cap_{graminoid}$ or cap_{moss} that accounts for drought stress in case the water table drops under a PFT-specific threshold (see section "Drought stress" below). In LPJ-GUESS-WHyMe, the growth of grasses and mosses is restricted by a PFT-specific maximum fpc. If the biomass of a PFT exceeds this threshold it is transferred to the litter pool. This is to account for the absence of nutrient limitation in the model and to assure coexistence of mosses and graminoids. In this study, fpc_{max} was calibrated for mosses and graminoids.

Phenology

To account for plant growth throughout the season, the fraction of PAR that is used for photosynthesis is multiplied by a factor φ that stands for daily phenology (see section "NPP and plant growth"). φ =0 corresponds to no photosynthesizing leave tissue and φ =1 corresponds to the maximum amount of photosynthesizing tissue/full leave-out. The daily phenology φ_n for day n depends on the number of growing degree days (GDD), which for day n is calculated as follows:

$$GDD_n = \sum_{i=1}^{n} \max\,(0, (T_i - T_{base}))$$

The standard T_{base} in LPJ-GUESS is 5 °C for all PFTs. In this study T_{base} was set to 0 °C as Euskirchen et al. (2014) found that for high arctic plants this led to more accurate predictions of phenology. Each PFT is characterized by a parameter GDD_{max} which is the number of GDD at which full leaf-out is reached.

$$\varphi_n = \min\left(1, \frac{GDD_n}{GDD_{max}}\right)$$

In this study, GDD_{max} for graminoids was estimated by calculating the number of GDD with T_{base} = 0°C until the peak value of measured GPP was reached, which was 170 GDD. GDD_{max} for mosses was set to 0, as mosses do not shed leaves over winter.

Water stress

Daily NPP for wetland PFTs is multiplied by a factor cap_{moss} or cap_{gram} to be reduced if the water table position drops below a PFT-specific threshold (wtp is negative when below the surface):

$$cap_{moss} = \begin{cases} 1 & if\ wtp > 0\ cm \\ 1 + wtp * \left(\frac{1 - cap_{\ moss,min}}{280}\right) & if\ 0\ cm > wtp \geq -280\ cm \\ cap_{\ moss,min} & if\ wtp \leq -280\ cm \end{cases}$$

$cap_{\ moss,min}$ was calibrated in this study and had been set to 0.3 in the original version (see section 2.4),

$$cap_{gram} = \min\left(\frac{wtp + 300\ cm}{f_{gram}}, 1\right)$$

f_{gram} was calibrated in this study and had been set to 200 cm in the original version.

2.3.3 Methane

The CH_4 routine of LPJ-GUESS-WHyMe consists of four steps: 1. Creation of a carbon pool within the soil carbon that is potentially available as a substrate for methanogenesis. 2. Methanogenesis and and other forms of decomposition, weighted depending on soil moisture in each soil layer. 3. CH_4 oxidation. 4. Transport of CH_4 to the atmosphere via diffusion, vascular plant transport and ebullition. Carbon emitted as methane does not contribute to NEE.

Potential carbon pool for methanogenesis

The first step of the CH_4 module is the creation of carbon pool that is potentially available as substrate for methanogenesis (see Figure 5). Carbon from dead plants or plant material (due to mortality or leaf/root turnover) is converted into a litter pool. The carbon from the litter pool is then distributed at a rate k_{litter} to a fast and a slow soil carbon pool and a substrate pool that is potentially available for methanogenesis. A fraction f_{atm} =0.7 is transferred directly into the potential carbon pool for methanogenesis. A fraction f_{fast}= 0.985 of the remaining litter carbon is allocated to the fast soil carbon pool, which has a faster turnover rate k_{fast}, according to which it is then transferred into the carbon pool potentially available for methanogenesis. A fraction $f_{slow} = 1 - f_{fast}$ is allocated to the

slow soil carbon pool, which has a slower turnover rate k_{slow}. Additionally, a fraction f_{exu} of NPP is allocated to root exudates, which have high content of substrate available to methanogens (see section 1.1.5). For this study, f_{exu} was derived from experiments (see section 2.2.3) and set to 6.4 %. Carbon from the exudates pool is transferred to the potential carbon pool for methanogens at a rate k_{exu}. The potential carbon pool for methanogens is distributed to the layer of the soil column weighted by the root distribution of vascular plants.

The turnover rates k_{litter}, k_{fast}, k_{slow} and k_{exu} all depend on a temperature-dependent factor R_T and a moisture dependent factor R_{moist}:

$$k_x = k_x^{10} R_T R_{moist} ,$$

where x stands for litter/fast/slow/atm/exu and k_x^{10} is the turnover rate at 10 °C. In the non-peatland version of LPJ-GUESS, R_{moist} depends on soil moisture and higher soil moisture leads to higher rates of decomposition. For inundated soils however, this relationship is not valid, as decomposition is slower under inundated conditions, so in LPJ-GUESS-WHyMe R_{moist} is set to a constant value so that turnover rates are reduced. In this study, R_{moist} was calibrated, as Wania et al. (2010) found it to be one of the three most important parameters controlling CH_4 emissions.

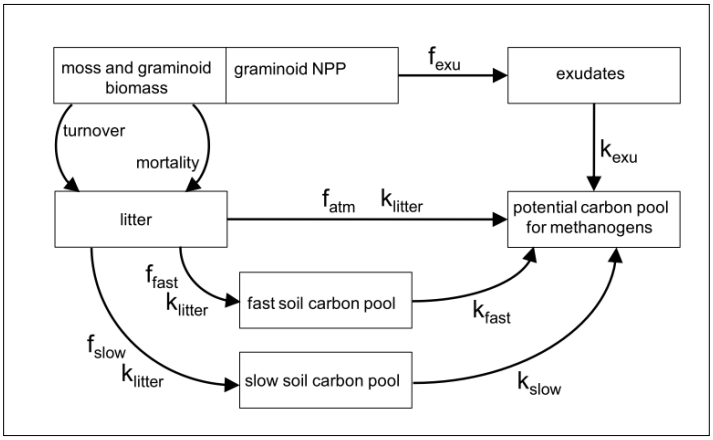

Figure 5: Conceptual diagram of the carbon pools and turnover rates involved in the creation of the potential substrate pool for methanoges.

Methanogenesis and other forms of decomposition

The carbon from the potential carbon pool for methanogens in each layer is turned partly into CH_4 and partly into CO_2 each day, depending on the O_2 content of the soil layer and a factor (CH_4/CO_2). The ratio (CH_4/CO_2) accounts for the fact that a fraction of the carbon pool available for methanogenesis is used by microorganisms that use alternative electron acceptors for anaerobic decomposition (see section 1.1.5) and thus differs between sites, depending on the availability of alternative electron acceptors. Wania et al. (2010) found the ration (CH_4/CO_2) to be one of the three most important parameters controlling CH_4 emissions, so it was calibrated in this study.

Oxidation

LPJ-GUESS-WHyMe simulates diffusion and plant-mediated transport of O_2 to each soil layer. The simulation of diffusion and plant-mediated transport of O_2 follow the same formulation as the transport of CH_4 in time-steps of 1/10 of a day, which is described in the next section. It is assumed that in each time step a fraction f_{oxid} of the O_2 is used by methanotrophs to oxidize CH_4, and the rest is used by plant roots and microorganisms other than methanogens. In the oxidation process, two moles of O_2 are used to oxidize one mole of CH_4:

$$CH_4 + 2\,O_2 \rightarrow CO_2 + 2\,H_2O$$

As Wania et al. (2010) found f_{oxid} to be one of the three most important parameters controlling CH_4 emissions, it was calibrated in this study.

Transport

Diffusion of CH_4, CO_2 and O_2 through the soil column is modeled at a time step of 1/10 of a day by numerically solving the diffusion equation. The fraction of CH_4 of each soil layer that is transported through plant mediation depends on the total tiller area of all vascular plant tillers, the fraction of roots that can be found in that soil layer. Plant mediation from any soil layer is treated similarly as diffusion from the top soil layer into the atmosphere, so the CH_4 bypasses oxidation in the layers in between.

The tiller area for one tiller a_{tiller} is calculated as flows:

$$a_{tiller} = \Phi_{tiller}\,\pi\,r_{tiller}^2$$

where, Φ_{tiller} is the tiller porosity, which is set to 70% as a default value, and r_{tiller} is the tiller radius, which is set to 3.5 mm as a default value. There were no field measurements available for r_{tiller} in Rylekærene, but according to our estimation it was much lower than 3.5 mm and we set the parameter to 0.5 mm. To obtain the total tiller area per m², a_{tiller} is multiplied with the number of tillers per m^2, n_{tiller}, which is calculated as follows:

$$n_{tiller} = \frac{m_{leaf,gram}\,\varphi_{gram}}{m_{tiller}}$$

$m_{leaf,gram}$ is the total leaf carbon mass of the graminoid PFT at the end of the previous year, φ_{gram} is the daily phenology of graminoids (see section "Phenology") and m_{tiller} is the carbon mass of one average tiller. The default value for m_{tiller} is 0.22 gC. Here it was set to 0.015 gC, which was the average tiller mass derived from measurements of biomass and number of tillers in the control plots (see section 2.2.2).

When the volume of CH_4 in a layer exceeds a certain threshold, ebullition occurs and a fraction of the CH_4 is transferred directly to the atmosphere. This was never the case in this study.

2.3.4 Summary of all changes made to adapt LPJ-GUESS-WHyMe to conditions in Rylekærene

Table 3 shows a summary of all the parameters that were changed in the model compared to the standard version of LPJ-GUESS-WHyMe used in the study by McGuire et al. (2012).

Table 3: Overview of all parameters that were changed to adapt LPJ-WHyMe to Rylekærene. The default values are the ones used in McGuire et al. (2012).

Parameter name	**Description**	**Default value**	**Site-specific value**	**Motivation for change**
h_{runon}	factor multiplied to thawing energy	1.0	calibrated	To account for energy brought into the system through melt water in spring
r	External run-on/off (mm/day)	0.0	calibrated	Melt water from mountains in spring, see above
$f_{conversion}$	Conversion factor: kg carbon to kg biomass	0.45	0.44	Field measurements
T_{base}	GDD base temperature	5 °C	0 °C	Euskirchen et al. (2014)
$GDD_{max,gram}$		-	170 °C day	GDD until maximum GPP was measured in 2013
$GDD_{max,moss}$		30 °C day	0 °C day	Mosses don't shed leaves over the winter
	C:N mass ratio of biomass	40	27	Field measurements
	Leaf:root biomass ratio of graminoids	0.4	0.5	Lab experiment by Falk et al. (2014)
$f_{graminoid}$	Factor in calculation of graminoids water stress (see section 2.3.2)	200	calibrated	Sensitivity to water stress is different in different species
$cap_{moss,min}$	Threshold in calculation of moss water stress (see section 2.3.2)	0.3	calibrated	Sensitivity to water stress is different in different species
$fpc_{max,gram}$	Maximum fractional projective cover of graminoids/mosses	0.864	calibrated	To account for N-limitation and disturbance
$fpc_{max,moss}$		0.632	calibrated	To account for N-limitation and disturbance
SLA_{moss}	Specific leaf area of mosses (m^2/kgC)	30	calibrated	To account for lower LUE of mosses and non-photosynthetic tissue
-	Inundation duration after which mosses die	15 days	31 days	No information on inundation tolerance of moss species available and the simulated wtp is potentially inaccurate in some years, so we decided not to include the process of moss death through inundation
	Fraction of NPP that graminoids allocate to root exudates in %	17.5	6.4	Estimation based on Ström et al. (2003) and Ström and Christensen (2007), see section 2.2.3
m_{tiller}	Tiller weight of graminoids (gC/tiller)	0.22	0.015	Average of measurements in exclosure experiment
r_{tiller}	Tiller radius of graminoids (mm)	3.5	0.5/calibrated	Estimation
R_{moist}	Moisture response of decomposition	0.4	calibrated	Site-specific parameters; these three parameters were the most important controls of CH4 emissions in Wania et al. (2010)
(CH_4/CO_2)	Fraction methanogenesis/CO_2 production under anaerobic conditions	0.25	calibrated	
f_{oxid}	Fraction of O_2 that is used for methane oxidation	0.9	calibrated	

2.4 Parameter calibration and validation

For calibrating parameters, the model was run multiple times with different sets of parameters, following a three-step calibration scheme (see Figure 6), that has not been used in other studies before. First, the parameters related to hydrology and permafrost dynamics ($h_{run\text{-}on}$ and r) were calibrated. Assuming that these processes were not affected significantly by vegetation and CH_4 dynamics in the model, the parameters related to vegetation and CH_4 were kept at the original LPJ-GUESS-WHyMe values as presented in Table 3. Then, the set of parameters that best reproduced measured active layer depth, soil temperature (T_{soil}) at 10 cm depth and water table position was chosen and set for the rest of the study. Secondly, parameters related to vegetation (SLA_{moss}, $fpc_{max,gram}$, $fpc_{max,\ moss}$, f_{gram} and $cap_{moss,\ max}$) were calibrated and thirdly parameters related to CH_4 dynamics

In each step, the best set of parameters was chosen by comparing the model output to field data from 2013 through the calculation of the root mean square error (RMSE, formula see below) and validated with field data from 2011. The reason for choosing to use 2013 as calibration year was that we had field data on biomass in 2013 but not in 2011. Each model run took about one minute, so we chose to calibrate a maximum of five parameters at the same time and to partition the parameters into three groups which were calibrated separately in three steps (see Figure 6). Table 4 shows the values for all parameters that were used to calibrate the model. The range was chosen by conducting some manual test-runs of the model.

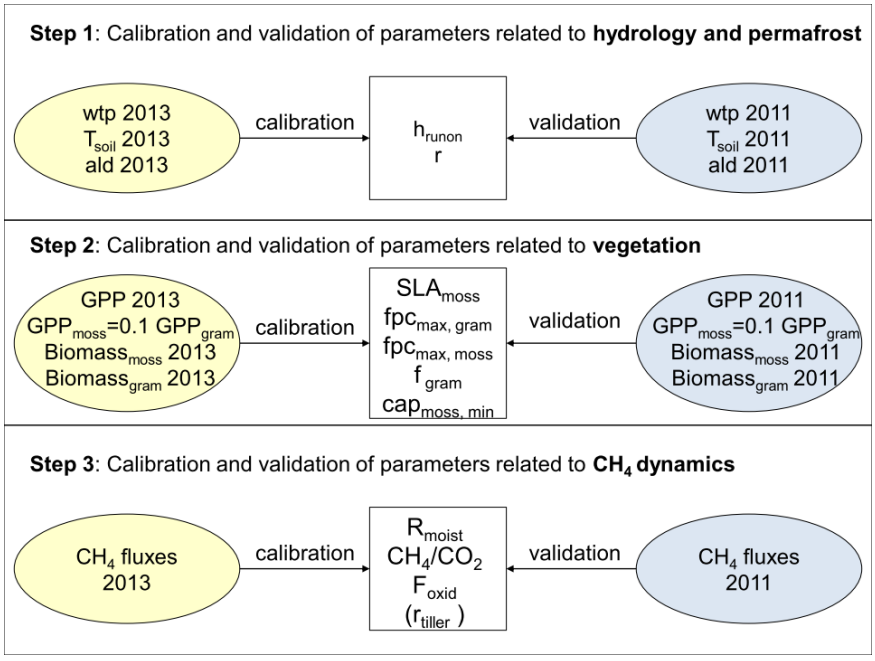

Figure 6: Schematic illustration of the three steps of the calibration and validation procedure.

Table 4: Values used for parameter calibrations.

	Parameter	Values that were used for parameter calibration										
Step 1	h_{runon}	5.0	5.5	6.0	6.5	7.0	7.5	8.0	8.5	9.0	9.5	10.0
	r	0.0	-0.1	-0.2	-0.3	-0.4	-0.5	-0.6	-0.7	-0.8	-0.9	-1.0
Step 2	SLA_{moss}	3	4	5	6	7						
	$fpc_{max,gram}$	0.1	0.15	0.2	0.25	0.3						
	$fpc_{\ max,moss}$	0.3	0.4	0.5	0.6	0.7						
	f_{gram}	100	200	300								
	$cap_{\ moss,min}$	0.3	0.65	1.0								
Step3a	R_{moist}	0.3	0.4	0.5	0.6	0.7						
	(CH_4/CO_2)	0.1	0.15	0.2	0.25	0.3	0.35	0.4				
	f_{oxid}	0.5	0.6	0.7	0.8	0.9						
Step 3b	r_{tiller}	1	2	3	4							

For comparison with the measured data, averages were computed from the daily model results that correspond to the averages that were computed from the measurements throughout the season in all the five plots (see section 2.2.2). For choosing the best set of parameters, the RMSE was calculated as follows (Smith and Smith 2007) for each model run:

$$RMSE = \frac{1}{\bar{O}} \cdot \sqrt{\frac{\sum_{i=1}^{n}(O_i - P_i)^2}{n}}$$

$\bar{O}$ is the average value of all the measurements, O_i is the ith measurement value, P_i is the ith modeled value and n is the total number of measured values.

For step one, the set of parameters which yielded the lowest value of $RMSE_{overall} = (RMSE_{ald} + RMSE_{soiltemp} + RMSE_{wtp})/3$ was chosen as the best set of parameters.

For step two, several RMSE were calculated:

$$RMSE_{overall} = (RMSE_{GPP} + RMSE_{moss\ biomass} + RMSE_{graminoid\ biomass} + RMSE_{NPP\ ratio\ moss:total\ vegetation})/4$$

$$RMSE_{gram} = (RMSE_{GPP} + RMSE_{graminoid\ biomass})/2$$

$$RMSE_{biomass} = (RMSE_{moss\ biomass} + RMSE_{graminoid\ biomass})/2$$

For the following studies of CH_4 dynamics, the parameter set yielding the lowest $RMSE_{gram}$ was used, as graminoids play an important role for CH_4 dynamics, while mosses do not influence CH_4 dynamics as much as graminoids in the model.

For step three, the set of parameters which yielded the lowest value of $RMSE_{CH_4}$ was determined. As the results pointed towards an underestimation of plant-mediated CH_4-emissions, the model was re-calibrated by also including graminoid tiller radius r_{tiller} as a calibrated parameter.

2.5 Sensitivity analysis

2.5.1 Sensitivity of vegetation

To evaluate the effect of fpc_{max} on graminoids and moss biomass, the model was run for all possible combinations of $fpc_{max,gram}$ (from 0.1 to 0.8 in steps of 0.05) and $fpc_{max,moss}$ (from 0.1 to 0.8 in steps of 0.05) and the effect on moss and graminoids biomass was evaluated. This procedure was done both for the set of vegetation parameters that yielded the lowest $RMSE_{overall}$, as well as for the parameter set that yielded the lowest $RMSE_{gram}$.

Also the sensitivity of graminoid and moss biomass to changes in the fraction of NPP allocated to root exudates (f_{exu}) was tested by running the model for values of f_{exu} ranging from 0 to 20% in steps of 0.5%. Again the analysis was performed both with set of vegetation parameters that yielded the lowest $RMSE_{overall}$, as well as for the parameter set that yielded the lowest $RMSE_{gram}$. This was done to see whether a higher f_{exu} would give graminoids a competitive disadvantage in the model.

2.5.2 Sensitivity of CH_4 dynamics

For analyzing the sensitivity of CH_4 fluxes, the model was run with the vegetation parameter set optimized for $RMSE_{gram}$.

The sensitivity of CH_4 fluxes to f_{exu} was tested by running the model multiple times while varying f_{exu} from 0% to 20% in steps of 0.5%. In a second step, the sensitivity of CH_4 fluxes to r_{tiller} was tested by running the model multiple times while varying r_{tiller} from 0.5mm to 10mm in steps of 0.5mm. 10mm is an unrealistically high value, but it was chosen to compensate for possible errors in tiller weight and tiller porosity, which are used in the same equation.

2.6 Musk-ox exclosure module

Simulating the effects of three years of musk-ox exclosure was limited in this study to simulating the changes in tiller density as observed in the field as well as the changes in root exudates as derived from the changes in vascular plant species composition (see section 2.2.3) for the last three years. Thus, f_{exu} was reduced from 6.2% to 5.4% for the last three years of the modeling period and the

parameter tiller weight was increased by 43 % (along with the reduced number of tillers in exclosure plots compared to control plots as measured in the field, see section 2.2.2), from 0.015 gC/tiller to 0.021 gC/tiller

3. Results

3.1 Climate and snow depth

Figure 8 shows time series from the CRU dataset and from measurements taken at the Zackenberg meteorological station of monthly mean temperature and monthly precipitation for the years 2000 to 2012. Linear regression (see Figure 7) led to the relationship $T_{Zack}=T_{CRU}*1.07+0.77$ ($R^2=0.97$), so this function was applied to T_{CRU} for the rest of the study. A linear regression of the relationship between monthly precipitation gave no linear relationship ($R^2=0.17$, see Figure 7), so precipitation CRU data was not modified.

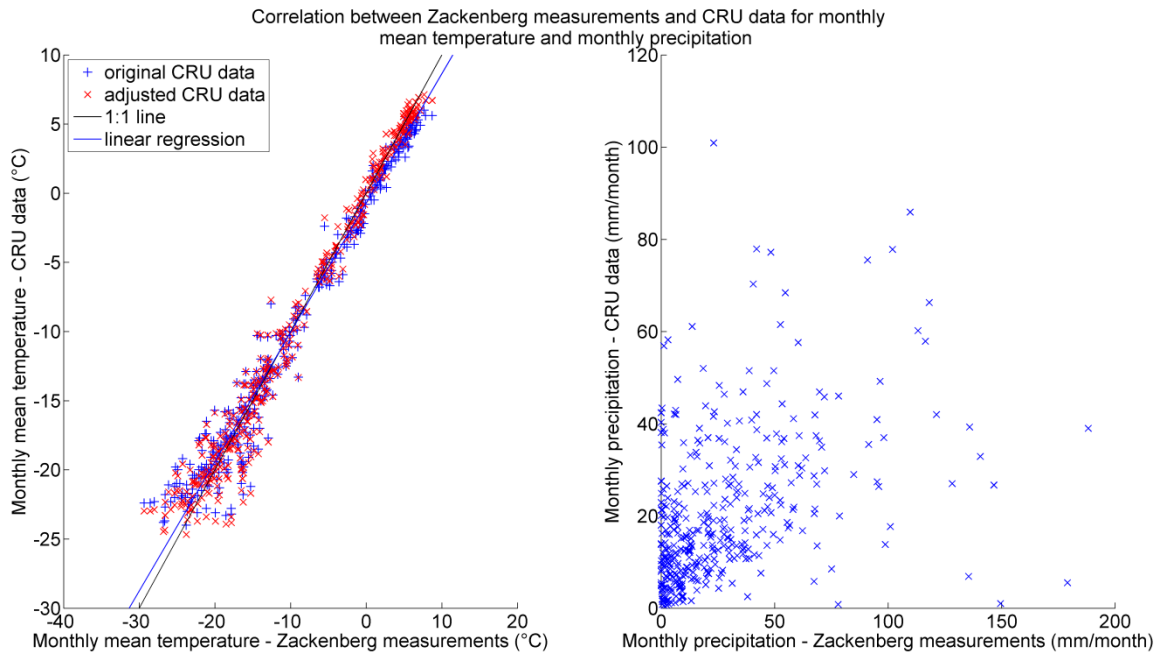

Figure 7: Monthly mean CRU temperature plot against monthly mean temperature as measured at the Zackenberg meteorological station and monthly CRU precipitation plot against monthly precipitation as measured at the Zackenberg meteorological station.

Figure 8 shows a time series of modeled and measured snow depth from 1997 to 2014. The seasonal pattern is similar in modeled snow depth, but in some years (e.g. 2002 and 2008) measured snow depth is much higher than modeled snow depth.

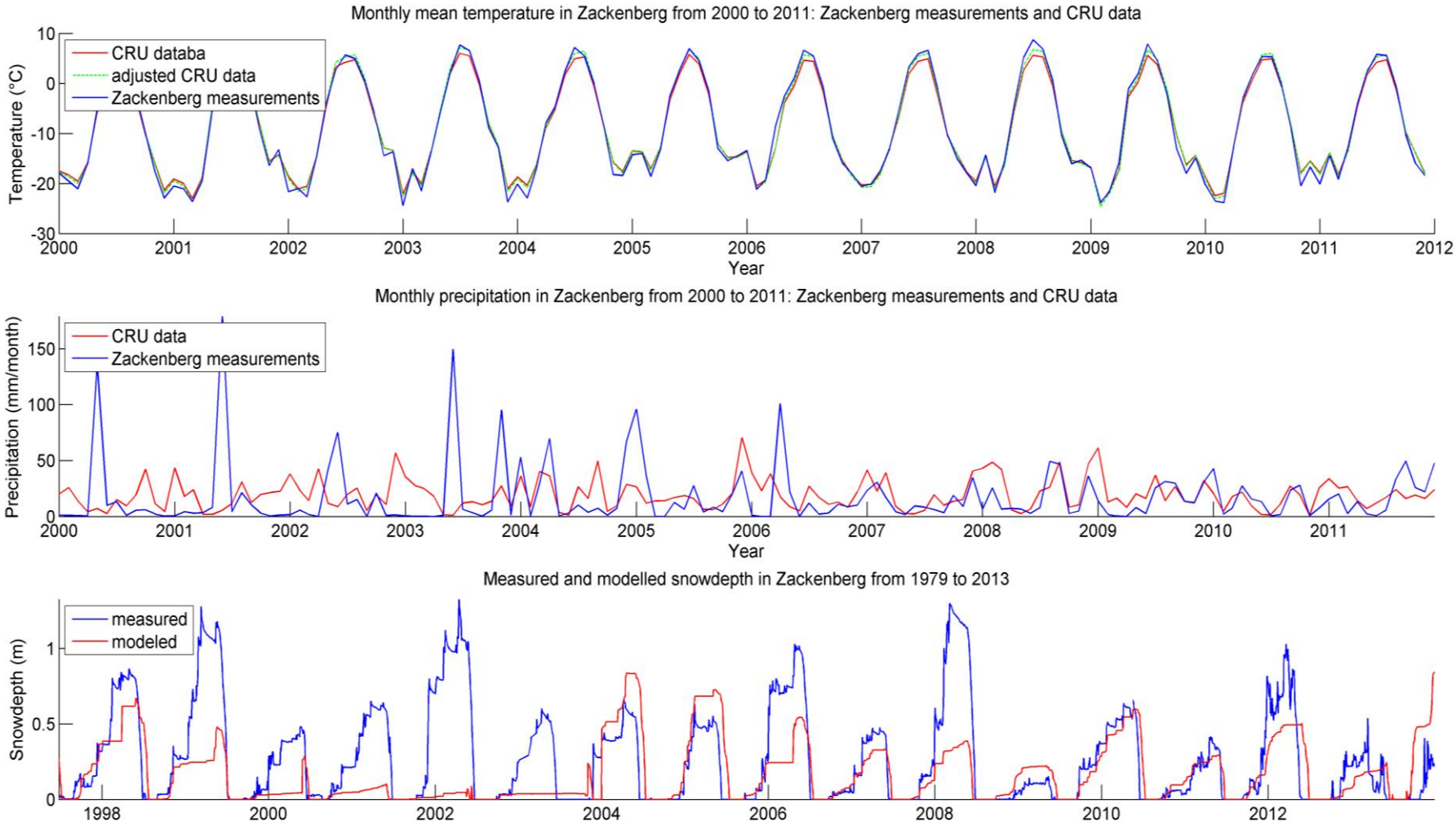

Figure 8: Time series of monthly mean temperature (Zackenberg measurements and CRU data), monthly precipitation (Zackenberg measurements and CRU data) and measured and modeled snow depth. The adjusted CRU data was obtained through a linear regression (see above).

3.2 Calibration and validation of parameters related to hydrology and permafrost

Results from the calibration and validation of the parameters related to hydrology and permafrost are presented in Figure 9 and Table 5. The best overall parameter set consisted of $h_{run\text{-}on}$ =5.5 and r = -0.8 mm/day. Using the best overall set of parameter decreased $RMSE_{total}$ from 0.77 to 0.28 compared to the default set and also decreased each of the RMSE for ald, T_{soil} and wtp for the calibration year 2013 (see Table 5). The set of parameters that minimized RMSE for ald was the same that reduced RMSE for T_{soil}.

For the validation year 2011 using the parameters optimized for 2013 reduced $RMSE_{total}$ from 0.94 to 0.71 (see Table 5), so the calibration improved performance for the validation year, but the model performed considerably better for the calibration period than for the validation period, especially for wtp ($RMSE_{wtp}$=1.05 for optimized parameter set).

The model underestimated soil temperature in the beginning of the growing season compared to measured data both in 2013 and 2011.

Modeled ald and T_{soil} using the overall best parameter set, the parameter set optimized for ald, while wtp was higher using the parameter set optimized for ald than when using the other parameter sets (see Figure 9).

Table 5: RMSE for default and calibrated parameter sets of $h_{run\text{-}on}$ and r for calibration year 2013 and validation year 2011.

year	parameter set	parameters		RMSE			
		$h_{run\text{-}on}$	**r**	**ald**	**T_{soil}**	**wtp**	**total**
2013	**default**	1.0	0.0	0.78	0.53	1.01	0.77
	overall optimized	5.5	-0.8	0.24	0.34	0.25	0.28
	optimized for ald	10	-0.4	0.20	0.31	0.73	0.41
	optimized for T_{soil}	10	-0.4	0.20	0.31	0.73	0.41
	optimized for wtp	9	-0.8	0.46	0.33	0.25	0.35
2011	**default**	1.0	0.0	0.81	0.65	1.37	0.94
	optimized for ald, T_{soil} and wtp	5.5	-0.8	0.61	0.49	1.05	0.71

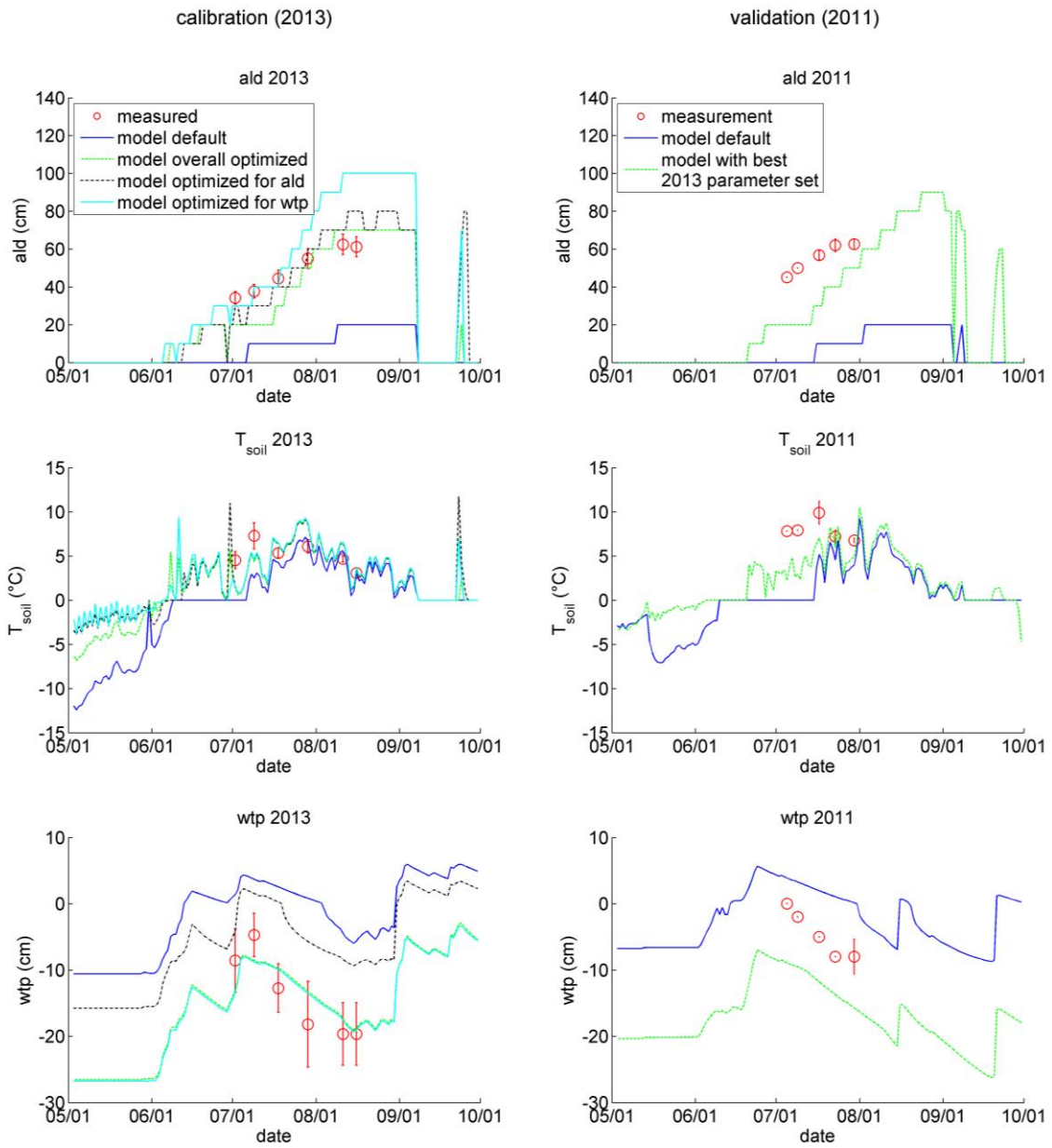

Figure 9: Measured and modeled values for active layer depth (ald), soil temperature at 10 cm depth (T_{soil}) and water table position (wtp) in the growing season of 2013 and 2011. For 2013, the modeled values shown include a run with the default parameter set and runs with the parameter sets that yield the best fit for ald, for wtp and for both. For 2011, the modeled values shown include a run with the default parameter set and a run with the parameter calibrated to fit ald and wtp for 2013.

3.3 Calibration and validation of parameters related to vegetation

With default vegetation parameters, modeled GPP and biomass differed substantially from measured values both in 2013 and 2011 (see Table 6 and Figure 10-13). $RMSE_{GPP}$ was as high as 1.16 in 2013 and 0.94 in 2011. There were no graminoids present in both years and GPP followed a pattern very different from the measured pattern. The calibration yielded an overall optimized vegetation parameter set of SLA_{moss}=3, $fpc_{max\ ,gram}$=0.3, $fpc_{max,\ moss=}$0.5, f_{gram}=200 and cap_{moss}=0.3, which is much lower values of fpc_{max} and SLA than the default parameter set, but the same values for f_{gram} and $cap_{moss,\ min}$. The best overall parameter set yielded a $RMSE_{total}$ of 0.29 for 2013 and 0.16 for 2011. The lower value for 2011 is partly due to the fact that there was no biomass data available for 2011.

The parameter set that performed best for GPP and graminoids biomass (SLA_{moss}=5, $fpc_{max,\ gram}$=0.3, $fpc_{max,moss}$=0.3, f_{gram}=300 and cap_{moss}=0.3) had a $RMSE_{tot}$=3.32, which is mostly due to the very high $RMSE_{NPP\ ratio\ moss:vegetation}$, and a $RMSE_{gram}$=0.16 for 2013. The parameter set that yielded the best $RMSE_{GPP}$ led to the absence of mosses. The parameter set that yielded the lowest $RMSE_{biomass}$ overestimated GPP and the ratio in NPP between mosses and total vegetation.

The pattern of GPP biomass and the ratio in NPP between mosses and total vegetation in the validation year 2011 looked fairly similar to the patterns of the calibration year 2013 in all parameter sets.

Table 6: RMSE for default and calibrated vegetation parameter sets for calibration year 2013 and validation year 2011.

		parameters					RMSE				
	year	**SLA** $_{moss}$	**fpc** $_{max,\ gram}$	**fpc** $_{max,\ moss}$	**f** $_{gram}$	**cap** $_{moss,\ min}$	**GPP**	**grami-noid biomass**	**moss bio-mass**	**moss NPP fraction**	**total**
default	2013 2011	30	0.86	0.63	200	0.3	1.14 0.94	-	0.65	- -	>0.9 >0.94
overall optimized	2013 2011	3	0.3	0.5	200	0.3	0.28 0.23	0.27	0.61	0.03 0.09	0.29 0.16
optimized for grami-noids bio-mass and GPP	2013 2011	5	0.3	0.3	300	0.3	0.35 0.34	0.01	0.25	9.35 11.0	3.32 5.67
optimized for GPP	2013 2011	4	0.3	0.2	200	1	0.15 0.22	0.27	1.0	1.0 1.0	0.61 0.61
optimized for grami-noids and moss bio-mass	2013 2011	4	0.3	0.3	300	1	0.65 0.53	0.02	0.07	14.5 17.8	3.81 9.17

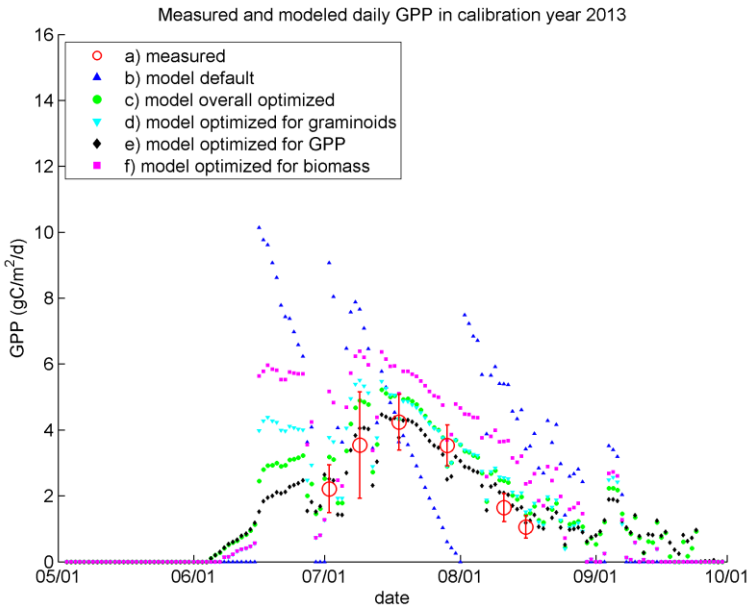

Figure 10: Measured (a)) and modeled GPP throughout the growing season of the calibration year 2013. The modeled values shown include a run with b) the default parameter set and runs with the parameter sets that yield the best fit for c) overall performance, d) graminoids biomass and GPP, e) GPP and f) graminoids and moss biomass.

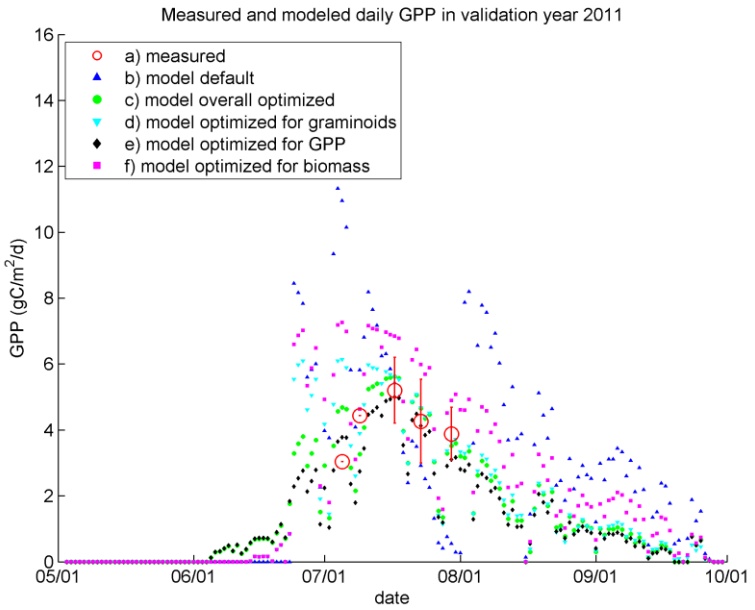

Figure 11: Measured (a)) and modeled GPP throughout the growing season of the validation year 2011. The modeled values shown include a run with b) the default parameter set and runs with the parameter sets that yield the best fit for c) overall performance, d) graminoids biomass and GPP, e) GPP and f) graminoids and moss biomass.

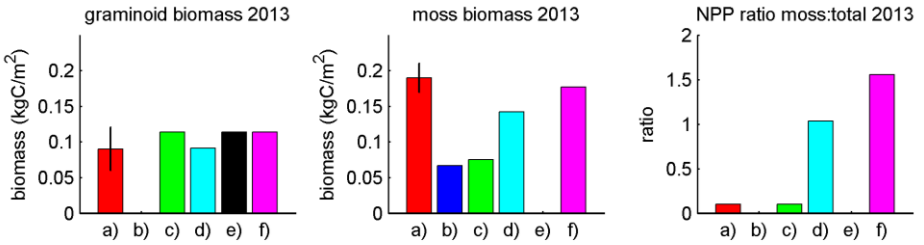

Figure 12: Graminoid biomass, moss biomass and the ratio between moss and total NPP for the calibration year 2013. The values include a) measured, b) model default, c) overall optimized, d) optimized for GPP and graminoids, e) optimized for GPP, f) optimized for graminoids and moss biomass values.

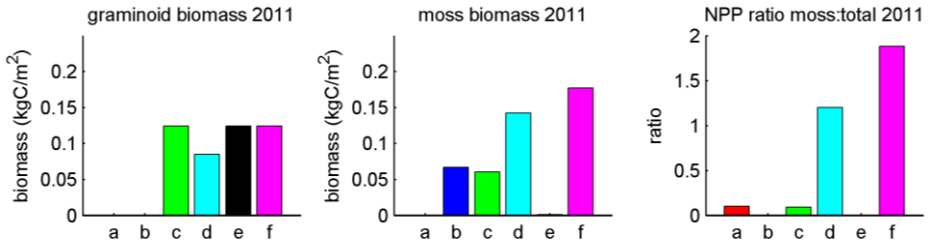

Figure 13: Graminoid biomass, moss biomass and the ratio between moss and total NPP for validation year 2011. The values include a) measured, b) model default, c) overall optimized, d) optimized for GPP and graminoids, e) optimized for GPP, f) optimized for graminoids and moss biomass values.

3.4 Calibration and validation of parameters related to CH_4 dynamics

When setting r_{tiller} to 0.5mm, the best CH_4 parameter set (R_{moist}=0.3, (CH_4/CO_2)=0.1, f_{oxid}=0.9) decreased $RMSE_{CH4}$ from 2.2 to 0.65 compared to the default parameter set (see Table 7). In 2011 the RMSE was lower for the default parameter set ($RMSE_{CH4}$=0.23) than for the default parameter set ($RMSE_{CH4}$=0.66). Additionally calibrating r_{tiller} yielded the same values for R_{moist}, (CH_4/CO_2) and f_{oxid} and a value for r_{tiller} of 4 mm. It reduced RMSE in 2013 to $RMSE_{CH4}$=0.44 and in 2011 to $RMSE_{CH4}$=0.61. Also with r_{tiller} =4 mm in 2011 the RMSE was lower for the default parameter set ($RMSE_{CH4}$=0.16) than for the default parameter set ($RMSE_{CH4}$=0.61).

Figure 14 shows measured and modeled CH_4 fluxes from 2013 and 2011 from model runs with r_{tiller}=0.5 mm and r_{tiller}=4 mm. All modeled time series of fluxes exhibit two more or less pronounced main peaks: one due to plant transport early in the season and one due to diffusion later in the season. The field data exhibits only one peak in the middle of the season. Diffusion in the version with r_{tiller}=0.5 mm exhibits a high peak in late August, that is not present in the version with r_{tiller} =4.

Table 7: RMSE for default and calibrated CH_4 parameter sets for calibration year 2013 and validation year 2011.

Parameter set	**r_{tiller}**	**R_{moist}**	**CH4/CO2**	**f_{oxid}**	**$RMSE_{CH4}$ 2013**	**$RMSE_{CH4}$ 2011**
Default, r_{tiller}=0.5mm	0.5	0.4	0.25	0.9	2.20	0.23
Optimized, r_{tiller}=0.5mm	0.5	0.3	0.1	0.9	0.65	0.66
Default, calibrated r_{tiller}	4.0	0.4	0.25	0.9	2.04	0.16
Optimized, calibrated r_{tiller}	4.0	0.3	0.1	0.9	0.44	0.61

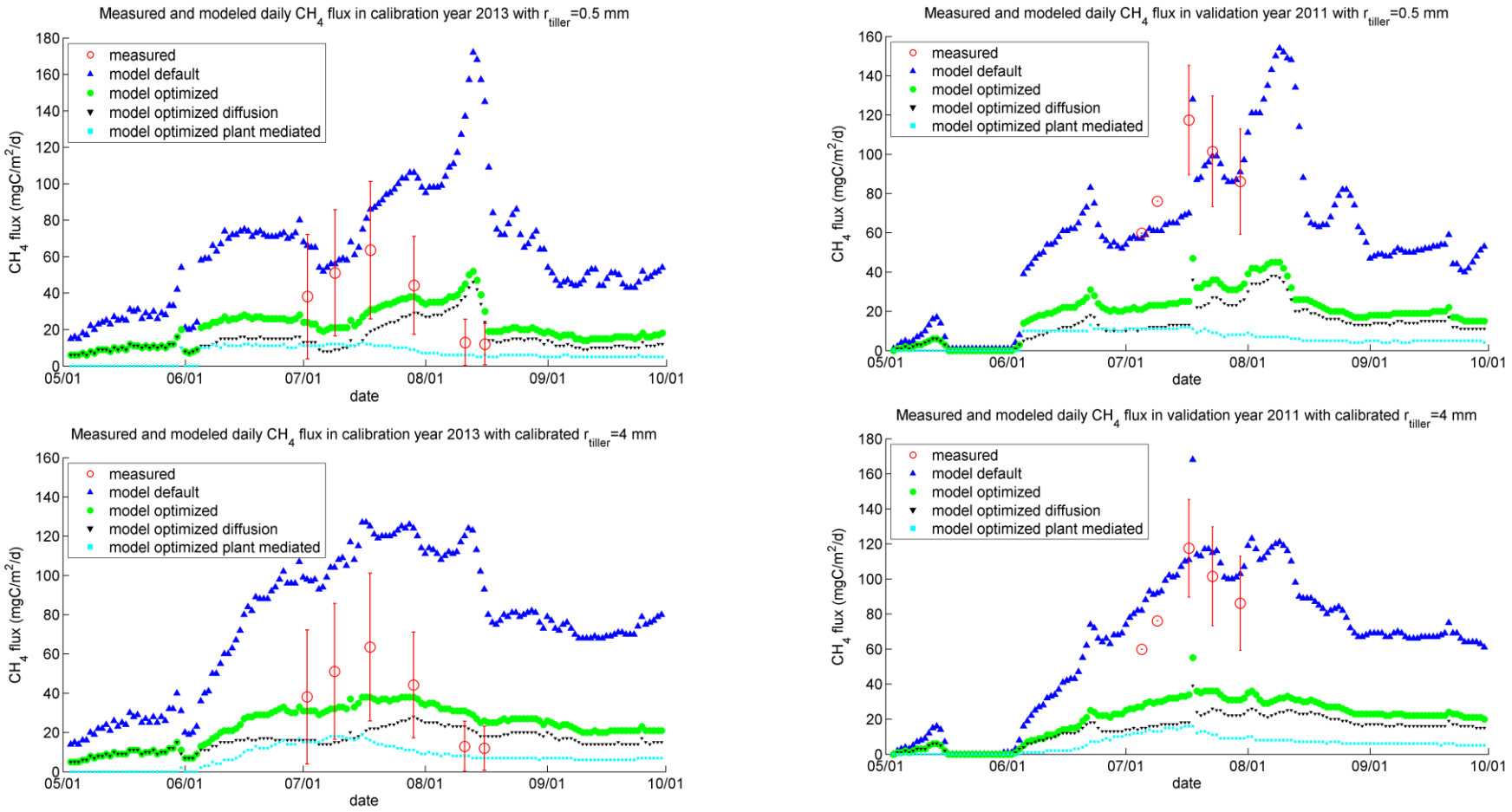

Figure 14: Measured and modeled daily CH_4 fluxes in the calibration year 2013 and the validation year 2011 with r_{tiller}= 0.5mm and calibrated r_{tiller}=4 mm. The modeled results shown include results from a model run with default CH_4 parameters and results from a run with optimized parameters, which is partitioned in diffusion and plant mediated transport.

3.5 Sensitivity analysis

3.5.1 Sensitivity of vegetation

Figure 15 shows moss and graminoid biomass in 2013 for combinations of $fpc_{max,\ moss}$ and $fpc_{max,\ gram}$, with $SLA_{moss,}$ f_{gram} and $cap_{moss,\ min}$ optimized for overall performance. Figure 16 shows the same for the parameter set optimized for GPP and graminoids biomass. It can be seen that in both cases graminoids biomass varies mostly smoothly along the parameter space: it increased with increasing $fpc_{max,gram}$ and is relatively constant with varying $fpc_{max,moss}$. Moss biomass spikes for some combinations of fpc_{max} and is zero for others and does not have a smooth, continuous variation like graminoids biomass.

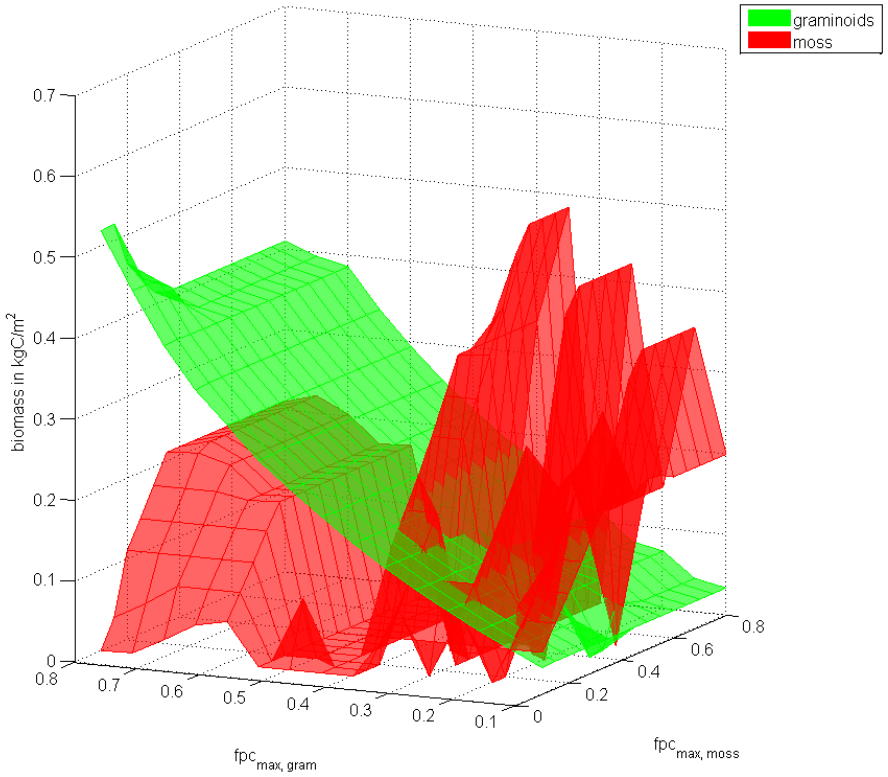

Figure 15: Moss and graminoid biomass in 2013 for combinations of $fpc_{max,\ moss}$ and $fpc_{max,\ gram}$, with $SLA_{moss,}$ f_{gram} and $cap_{moss,\ min}$ optimized for overall performance.

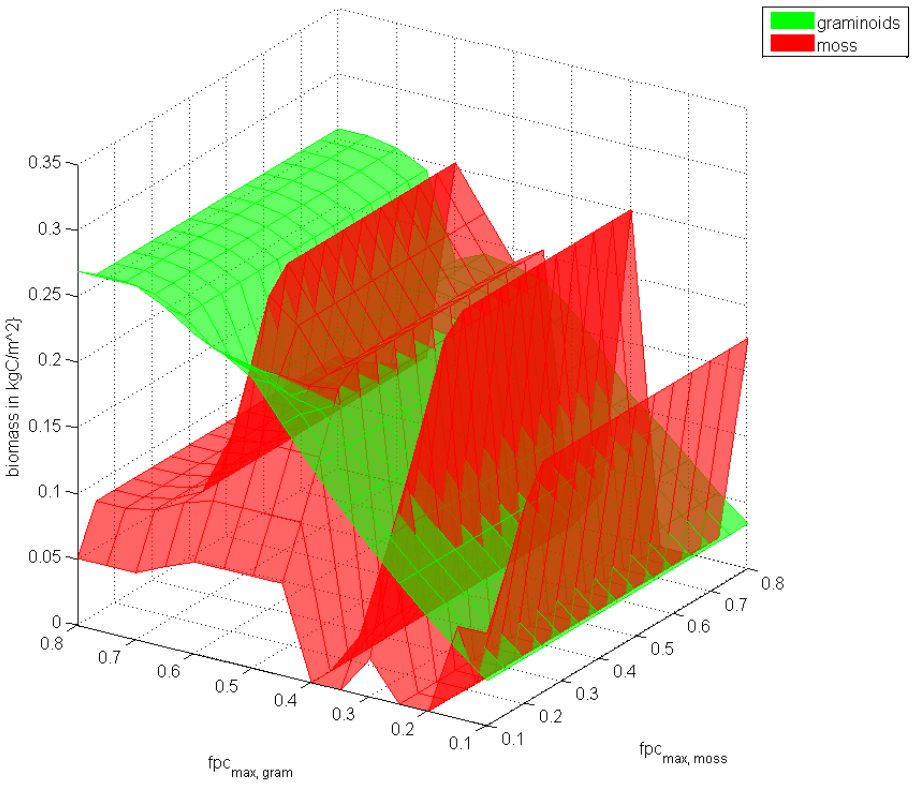

Figure 16: Moss and graminoid biomass in 2013 for combinations of $fpc_{max,\ moss}$ and $fpc_{max,\ gram}$, with SLA_{moss}, f_{gram} and $cap_{moss,\ min}$ optimized for graminoids biomass and GPP.

Varying f_{exu} had considerable effects on moss and graminoid biomass for both parameter sets. With the overall optimized parameter set graminoid biomass stayed almost constant, while moss biomass varied. For the set of vegetation parameters optimized for GPP and graminoids biomass, moss biomass stayed mostly constant, apart from a drop at around 15%. Graminoid biomass decreased with increasing f_{exu}, apart from a spike simultaneously with the drop in moss biomass.

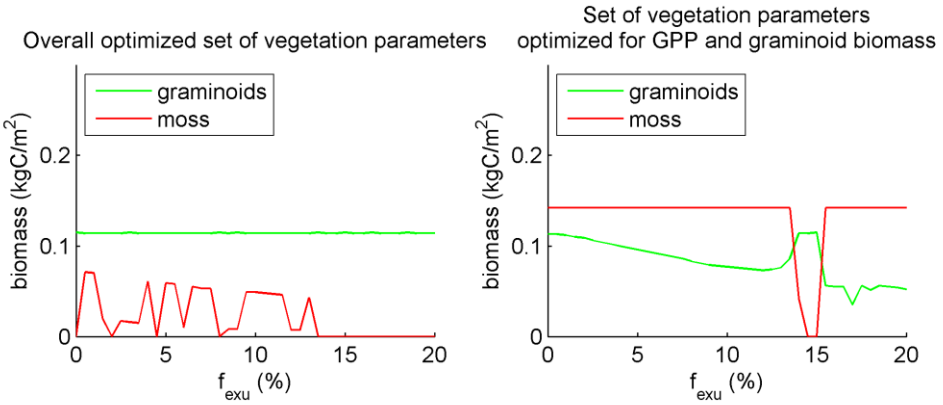

Figure 17: Graminoid and moss biomass in 2013 for model runs with varied f_{exu}.

3.5.2 Sensitivity of CH_4 dynamics

Varying f_{exu} and r_{tiller} both had considerable effect on CH_4 fluxes (see Figure 19). CH_4 fluxes were lowest for f_{exu} around 8% and higher for both lower and higher values of f_{exu}. The highest fluxes occurred at around 12% higher values of f_{exu} yielded lower CH_4 emissions.

Varying r_{tiller} had different effects on diffusion and on plant mediated fluxes. Diffusion was not affected much by r_{tiller} before July and then it was generally lower for lower values of r_{tiller}, with the exception of a high peak in early August for values of r_{tiller} between 0 and 4 mm. Plant mediated fluxes were affected by r_{tiller} both in timing and magnitude of peak emission. Plant mediated CH_4 emissions were highest for r_{tiller} around 4 mm and both higher and lower values of r_{tiller} yielded lower plant-mediated CH_4 emissions. For approximately r_{tiller}< 5mm, plant-mediated emissions peaked in mid-July, while for approximately r_{tiller}> 5mm plant-mediated emissions peaked in mid-June already, with a lower peak, and then declined quickly.

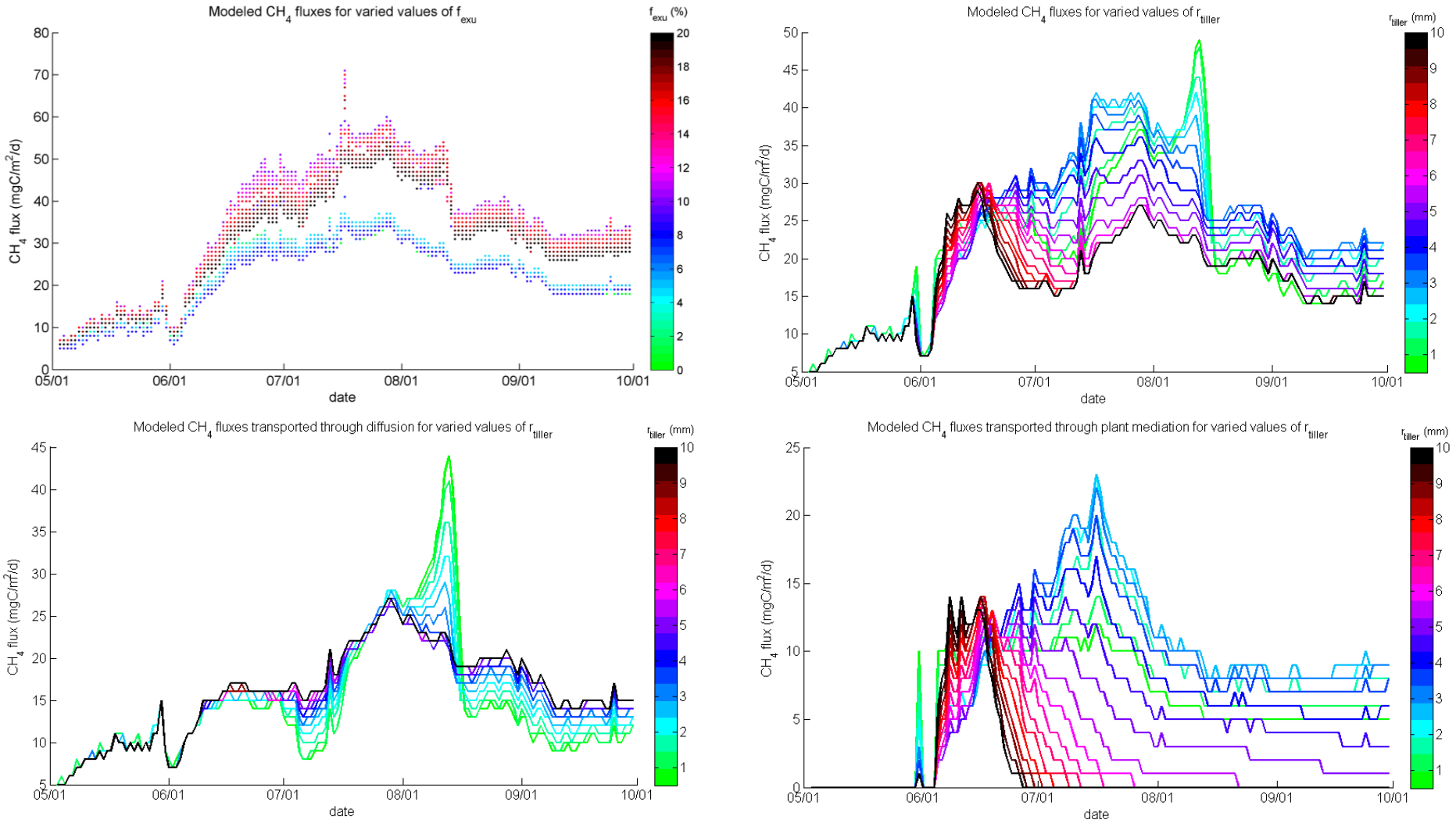

Figure 18: Modeled CH_4 fluxes in 2013 for different values of f_{exu} and r_{tiller}.

3.6 Musk-ox exclosure module

Figure 19 shows the effect of implementing the exclosure module for the last three years of the modelling period on CH_4 fluxes, as well as CH_4 fluxes from control and exclosure plots from the field. The difference in fluxes between control and exclosure plots was much larger in the field than in the model and it had opposite direction: In the field, fluxes were lower in the exclosure plots than in control plots, while in the model they were slightly higher.

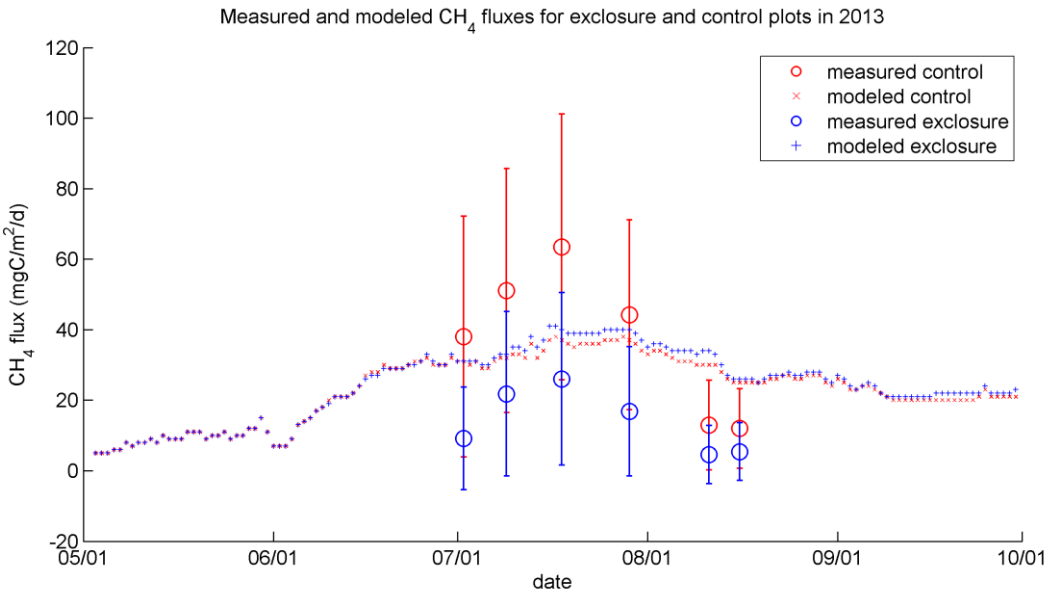

Figure 19: Measured and modeled CH_4 fluxes for exclosure and control plots in 2013.

4. Discussion

4.1 Climate and snowdepth

Temperatures from the CRU dataset were lower in summer and higher in winter than the temperatures measured at the Zackenberg meteorological station. This can be explained by the microclimate in the valley, which is different from the average climate in the gridcell of the CRU dataset. Cai (2014) compared site climate data for different wetland sites and found higher deviations than the deviation found in this study. For their northernmost site (Abisko, Sweden) they found a temperature offset of 3.22°C, which is considerably higher than the 0.77°C found in Zackenberg valley this study.

Precipitation differed much between the CRU dataset and Zackenberg measurements, but not with a systematic offset, so the usage of CRU precipitation data might be more problematic than the usage of CRU temperature data.

Microclimate plays an important role in the Arctic, so CRU data needs to be used carefully when modelling vegetation and carbon dynamics. In this study we used original site data for the last 35 years of the modelling period and analyzed only data from 2011 and 2013, so the usage of adjusted CRU data is probably not problematic. It would be interesting to test the sensitivity of the modeled vegetation and carbon fluxes to the climate forcing to determine how important accurate climate forcing is in comparison with model parameters.

For snow depth the model reproduced the seasonal pattern well, but in some years there were big differences in snow depth differences between model and measurements (see Figure 8). A reason for this could be that snow is affected by wind. However the measurements of snow depth were not taken directly at Rylekærene, but at a meteorological station close by, where the snow depth might differ. It would be interesting to evaluate the model's performance at predicting the date of snow melt, as date of snow melt has been shown to be a crucial factor for hydrology and CH_4 dynamics in Rylekærene (Mastepanov et al. 2013), but for doing so it would be better to use field data taken directly at the site.

4.2 Hydrology and permafrost

The model performed significantly better with adjustments using the parameters $h_{run\text{-}on}$ and r, especially for 2013. In 2011 the adjustments also improved model performance, but not as significantly. In 2011 there was slightly more snow than in 2013 (see Figure 8) and the soil temperature was higher in the beginning of the season 2011 than 2013 (see Figure 9). This indicated that there was more run-on/off in 2011 than in 2013, causing the poorer performance of the model in predicting T_{soil}, ald and wtp. Compared to other years, 2011 and 2013 had relatively similar amounts of snow during the preceding winter, so the approximation used in this study might not perform as well for years with differing snow conditions. The model underestimated soil temperatures in the beginning of the season of both years, which might be a problem for modeling CH_{fluxes}, but the

adjusted model performed better than the model with default settings. When Wania et al. (2010) applied LPJ-Why to a site in northern Sweden (the mire Stordalen in Abisko), they had the same situation as in Rylekærene: without the inclusion of melt water from the mountains the results were very different from field observations. Incorporating a topography-depending hydrology scheme like developed by Tang et al. (2014b) might solve these problems. However this hydrology scheme does not include the heat transfer connected to run-on/off yet, which is an important factor in Rylekærene. The approximation of the effects of run-on/off on the hydrology and soil temperatures used in this study could improve model performance in the study years without needing a topography-dependent hydrology scheme, which enabled us to study the modelling of vegetation and CH_4 dynamics with less errors in T_{soil} and wtp. However, these adjustments cannot be applied at other sites, and in Rylekærene they can only be applied as long as snow conditions and temperatures do not vary too much.

The best sets of parameters for ald and wtp, as well as the one best for both led to similar patterns of ald throughout the season. There was much more difference in wtp between these parameter sets. This indicates that accurate dynamics of active layer are very important for getting accurate dynamics of wtp. The best set of parameters for active layer depth is the same as the best set for soil temperature. This shows that the model is able to simulate soil thermal dynamics accurately.

Effects of moss on hydrology and soil temperature is currently not modeled, but might be substantial (Frolking et al. 2010). The calibrated parameters might compensate for this in part, but it is important to consider this for future studies.

4.3 Vegetation

By calibrating vegetation parameters we were able to reproduce GPP, graminoids and moss biomass and the ratio between moss NPP and total NPP successfully for the study years 2011 and 2013, so that a base was lain to reduce model uncertainty due to vegetation properties when modeling CH_4 dynamics.

The sensitivity study however showed that small changes in parameters like fpc_{max} and f_{exu} can lead to extreme shifts in modeled vegetation composition, especially in moss biomass (see Figure 15-17). The behavior of moss biomass while varying $fpc_{gram,max}$ or f_{exu} is very unrealistic. It is thus essential to improve both process representations of vegetation dynamics and PFT parametrization.

A big problem is that nutrient limitation is not included in the model, as the arctic tundra is very nutrient-limited (Jonasson et al. 1999). This is why we had to reduce fpc_{max} to very low values in order to not overestimate plant biomass. However, a module for nitrogen-dynamics has recently been developed for LPJ-GUESS (Smith et al. 2014), that could also be included in LPJ-GUESS-WHyMe.

Another problem is that in the formulation of light competition (see section 2.3.2) it is assumed that mosses and graminoids have similar shapes. It could be an improvement to simulate height of

graminoids and moss layer thickness explicitly and to include non-photosynthetic tissue in the representation of mosses. Modeling moss layer thickness would also be necessary for modeling its effect on soil temperature and hydrology.

Root exudates have complex functions, and can give competitive advantages to plants, for example by regulating pH (Javed et al. 2013). In the model, however, allocating a larger part of NPP to root exudates reduces NPP and is thus a competitive disadvantage for the plant. This needs to be considered especially when implementing several vascular plant PFTs.

There was some uncertainty in the comparison between field data on vegetation properties and modeled properties. One problem is the conversion between units of plant biomass, which is usually kg of dried biomass in the field and kgC in the model. The unit conversion used in this study was derived from measurements of graminoids biomass, so it would be helpful to measure carbon content of moss biomass as well. Another problem was that the sampled biomass included not only green biomass.

4.4 Methane

After the CH_4 parameter calibration the model was able to reproduce the magnitude of the CH_4 fluxes as measured in the field. However, it overestimated CH_4 fluxes in the beginning and the end of the growing season and underestimated CH_4 fluxes at peak growing season (see Figure 14). Plant transport in the model peaked too early, earlier than GPP. This pattern was also observed by Wania et al. (2010) when applying LPJ-WHyMe to northern peatlands, so this might be a problem common to northern sites. The calibration worsened model performance in 2011, which was much better with the default parameter set, so the parameters might change between years.

Field measurements in Rylekærene have shown strong correlations between vascular plant biomass/NPP and CH_4 fluxes (e.g. Ström et al. 2015) and this was confirmed by the seasonal pattern of measured CH_4 emissions in this study, which was similar to the seasonal pattern of GPP. The problems leading to the inaccurate seasonal variation of CH_4 could be the underestimation of plant transport due to inaccurate parametrization, the overestimation of diffusion, for example due to inaccurate soil porosity parametrization, or an inaccurate parametrization of root exudates.

The modeled CH_4 fluxes were sensitive to changes in r_{tiller} and f_{exu} (see Figure 18). The peak in August at low tiller radius might be caused by a build-up of CH_4 in the soil in the preceding period, as less CH_4 is released through plants due to the low tiller radius and less O_2 is transported into the soil through plants to be used in oxidation. Plant mediation declined quickly after a peak in June for high tiller radius >5mm. This could because of the increased transport of O_2 into the soil that comes with higher tiller areas, however diffusion did not decline for r_{tiller}>5 mm.

The sensitivity of plant biomass to f_{exu} and the finding that increasing f_{exud} may result in decreased CH_4 emissions imply that increasing the fraction of NPP allocated to root exudates decreases NPP as well, so that the net effect of increasing f_{exu} is not an increase, but a decrease in the soil root exudates pool.

The area around Rylekærene has recently been shown to be a regional net CH_4 sink (Jorgensen et al. 2015), so for larger-scale simulations it would be good to incorporate CH_4 dynamics also in the non-peatland version of LPJ-GUESS.

In this study, the model was evaluated using only data from six weekly averages throughout the growing season, but data from automatic chamber measurements (e.g. Mastepanov et al. 2013) could also be used.

4.5 Grazing

This thesis started out with the idea to implement a grazing module into LPJ-GUESS-WHyMe that can simulate the effect of grazing over longer time-periods dependent on herbivore density. However we came to the conclusion that the current mechanisms for modelling vegetation dynamics are not sufficiently detailed for implementing the impact of herbivores accurately. The most important step towards modeling the effects seen in the exclosure experiment would be to implement a more detailed scheme for light competition, as proposed in section 4.3.

Also the available data is not sufficient to draw conclusions on the interplay of the multiple mechanisms in which grazing affects the ecosystem and the data from three years of exclosure is not sufficient to draw conclusions on long-term effects of grazing on the ecosystem.

The simple exclosure module tested in this study (see section 3.6), which included a reduction in root exudation and in tiller density as observed in the field, had opposite and much lower effects on CH_4. This can be related to the problems in modelling the relationship between vascular plants and CH_4 dynamics accurately, as described above.

There have been two studies published on modelling grazing in the arctic so far (Yu et al. 2009; Yu et al. 2011), which implemented grazing by removing a part of the vascular plant biomass. In the mire studied, however, it has been shown that the net effect of grazing is an increase of vascular plant biomass and that trampling of mosses is an important (Falk et al. 2015), so solely removing vascular plant biomass would not be a good approach for modelling grazing in Rylekærene.

With more detailed process implementation and studies on long-term effects of herbivory, effects of trampling and manure it would be possible to build a grazing module that could model the effect of grazing on vegetation and carbon dynamics in Rylekærene and similar sites as a function of herbivore-densities. Trampling could be implemented in form of a reduction of moss layer thickeness (which

would also affect its thermal and hydrological properties), grazing as the removal of graminoid biomass, and manure could be incorporated as a pool in a N-cycling routine.

4.6 Suggestions for future research

The data collected in Rylekærene has great potential to be used for further improvements of process representations in wetland vegetation and carbon dynamics modelling, especially for improving the modeled relationship between graminoids abundance and CH_4 fluxes.

Data throughout the season of moss-only plots (Falk et al. 2014) could additionally be used to improve moss parametrization.

Additional data that would be useful to collect includes tiller area, thickness of moss layer and fraction of non-photosynthetic tissue in mosses. Also it would be helpful to conduct more studies that estimate root exudates fraction as a fraction of NPP.

It could also be considered to put some data (e.g. tiller height, tiller area, root exudates fractions, C and N content of the biomass) into the TRY trait database (Kattge et al. 2011), as currently it does not include any information on functional traits of the plant species that were present in Rylekærene.

5. Conclusion

In this study, for the first time, we used extensive field data from studies in the high Arctic mire Rylekærene to evaluate processes and parametrization of hydrology, soil temperature and permafrost dynamics within the wetland vegetation dynamic, hydrology and methane model LPJ-GUESS-WHyMe. The calibration procedure improved model performance for both calibration year 2013 and validation year 2011 for most of the outputs tested.

Main challenges for future studies were identified to be 1) modeling the effect of run-on/off from snowmelt 2) modeling competition between grasses and mosses and 3) modeling the effect of graminoid density on CH_4 fluxes accurately.

An important finding regarding CH_4 and vegetation dynamics was that increasing the fraction of NPP allocated to root exudates also decreased vascular plant productivity and thus had a net-effect of decreasing CH_4 emissions.

The possibility of implementing a grazing module into LPJ-GUESS-WHyMe was discussed and a simple prototype was tested. The most important step towards implementing a grazing module would be to implement a more detailed scheme for light competition between mosses and graminoids and to represent the effect of graminoid density on CH_4 fluxes accurately.

6. Acknowledgements

I would like to thank my supervisors Lena Ström and Paul Miller for helping and supporting me in my work and for their patience and Jing Tang for showing me how to run the model with multiple parameter combinations. I am very grateful to my family, friends and especially Juan for supporting me and keeping me sane at the times when I was close to getting lost in parameter space.

7. References

ACIA. 2005. *Arctic Climate Impact Assessment*. New York: Cambridge University Press.

Belshe, E. F., E. A. G. Schuur, and B. M. Bolker. 2013. Tundra ecosystems observed to be CO2 sources due to differential amplification of the carbon cycle. *Ecology Letters*, 16**:** 1307-1315. DOI: 10.1111/ele.12164

Berg, T. B., N. M. Schmidt, T. T. Hoye, P. J. Aastrup, D. K. Hendrichsen, M. C. Forchhammer, and D. R. Klein. 2008. High-arctic plant-herbivore interactions under climate influence. *Advances in Ecological Research, Vol 40*, 40**:** 275-298. DOI: 10.1016/s0065-2504(07)00012-8

Box, G. E. P., and N. R. Draper. 1987. *Empirical Model-Building and Response Surfaces*. Wiley.

Cahoon, S. M. P., P. F. Sullivan, E. Post, and J. M. Welker. 2012. Large herbivores limit CO2 uptake and suppress carbon cycle responses to warming in West Greenland. *Global Change Biology*, 18**:** 469-479. DOI: 10.1111/j.1365-2486.2011.02528.x

Cai, Z. 2014. Modelling methane emissions from Arctic tundra wetlands: effects of fractional wetland maps PhD Thesis. Lund: Lunds University

Christiansen, H. H., C. Sigsgaard, O. Humlum, M. Rasch, and B. U. Hansen. 2008. Permafrost and periglacial geomorphology at Zackenberg. *Advances in Ecological Research, Vol 40*, 40**:** 151-174. DOI: 10.1016/s0065-2504(07)00007-4

Cox, P. M., R. A. Betts, C. D. Jones, S. A. Spall, and I. J. Totterdell. 2000. Acceleration of global warming due to carbon-cycle feedbacks in a coupled climate model. *Nature*, 408**:** 184-187. DOI: 10.1038/35041539

Elberling, B., M. P. Tamstorf, A. Michelsen, M. F. Arndal, C. Sigsgaard, L. Illeris, C. Bay, B. U. Hansen, et al. 2008. Soil and plant community-characteristics and dynamics at Zackenberg. *Advances in Ecological Research, Vol 40*, 40**:** 223-248. DOI: 10.1016/s0065-2504(07)00010-4

Euskirchen, E. S., T. B. Carman, and A. D. McGuire. 2014. Changes in the structure and function of northern Alaskan ecosystems when considering variable leaf-out times across groupings of species in a dynamic vegetation model. *Global Change Biology*, 20**:** 963-978.

Falk, J. M., N. M. Schmidt, T. R. Christensen, and L. Ström. 2015. Large herbivore grazing affects the vegetation structure and greenhouse gas balance in a high arctic mire. *Environmental Research Letters*, 10.

Falk, J. M., N. M. Schmidt, and L. Ström. 2014. Effects of simulated increased grazing on carbon allocation patterns in a high arctic mire. *Biogeochemistry*, 119**:** 229-244. DOI: 10.1007/s10533-014-9962-5

Farquhar, G. D., S. V. Caemmerer, and J. A. Berry. 1980. A BIOCHEMICAL-MODEL OF PHOTOSYNTHETIC CO2 ASSIMILATION IN LEAVES OF C-3 SPECIES. *Planta*, 149**:** 78-90. DOI: 10.1007/bf00386231

Farquhar, G. D., and T. D. Sharkey. 1982. STOMATAL CONDUCTANCE AND PHOTOSYNTHESIS. *Annual Review of Plant Physiology and Plant Molecular Biology*, 33**:** 317-345. DOI: 10.1146/annurev.pp.33.060182.001533

Forchhammer, M. C., N. M. Schmidt, T. T. Hoye, T. B. Berg, D. K. Hendrichsen, and E. Post. 2008. Population dynamical responses to climate change. *Advances in Ecological Research, Vol 40*, 40**:** 391-419. DOI: 10.1016/s0065-2504(08)00017-7

Frolking, S., N. T. Roulet, E. Tuittila, J. L. Bubier, A. Quillet, J. Talbot, and P. J. H. Richard. 2010. A new model of Holocene peatland net primary production, decomposition, water balance, and peat accumulation. *Earth System Dynamics*, 1**:** 1-21. DOI: 10.5194/esd-1-1-2010

Gerten, D., S. Schaphoff, U. Haberlandt, W. Lucht, and S. Sitch. 2004. Terrestrial vegetation and water balance - hydrological evaluation of a dynamic global vegetation model. *Journal of Hydrology*, 286**:** 249-270. DOI: 10.1016/j.jhydrol.2003.09.029

Hansen, B. U., C. Sigsgaard, L. Rasmussen, J. Cappelen, J. Hinkler, S. H. Mernild, D. Petersen, M. P. Tamstorf, et al. 2008. Present-day climate at Zackenberg. In *Advances in Ecological Research, Vol 40: High-Arctic Ecosystem Dynamics in a Changing Climate*, eds. H. Meltofte, T. R. Christensen, B. Elberling, M. C. Forchhammer, and M. Rasch, 111-149 pp. San Diego: Elsevier Academic Press Inc.

Harris, I., P. D. Jones, T. J. Osborn, and D. H. Lister. 2014. Updated high-resolution grids of monthly climatic observations - the CRU TS3.10 Dataset. *International Journal of Climatology*, 34**:** 623-642. DOI: 10.1002/joc.3711

Haxeltine, A., and I. C. Prentice. 1996. BIOME3: An equilibrium terrestrial biosphere model based on ecophysiological constraints, resource availability, and competition among plant functional types. *Global Biogeochemical Cycles*, 10**:** 693-709. DOI: 10.1029/96gb02344

IPCC. 2013. *Climate Change: The Physical Science Basis. Working group I contribution to the IPCC fifth Assessment, Report (AR5)*, . Cambridge, United Kingdom and New York, NY, USA: Cambridge University Press.

Javed, M. T., E. Stoltz, S. Lindberg, and M. Greger. 2013. Changes in pH and organic acids in mucilage of Eriophorum angustifolium roots after exposure to elevated concentrations of toxic elements. *Environmental Science and Pollution Research*, 20**:** 1876-1880. DOI: 10.1007/s11356-012-1413-z

Jonasson, S., A. Michelsen, and I. K. Schmidt. 1999. Coupling of nutrient cycling and carbon dynamics in the Arctic, integration of soil microbial and plant processes. *Applied Soil Ecology*, 11**:** 135-146. DOI: 10.1016/s0929-1393(98)00145-0

Jorgensen, C. J., K. M. L. Johansen, A. Westergaard-Nielsen, and B. Elberling. 2015. Net regional methane sink in High Arctic soils of northeast Greenland. *Nature Geoscience*, 8**:** 20-23. DOI: 10.1038/ngeo2305

Kattge, J., S. Diaz, S. Lavorel, C. Prentice, P. Leadley, G. Bonisch, E. Garnier, M. Westoby, et al. 2011. TRY - a global database of plant traits. *Global Change Biology*, 17**:** 2905-2935. DOI: 10.1111/j.1365-2486.2011.02451.x

Kristensen, D. K., E. Kristensen, M. C. Forchhammer, A. Michelsen, and N. M. Schmidt. 2011. Arctic herbivore diet can be inferred from stable carbon and nitrogen isotopes in C-3 plants, faeces, and wool. *Canadian Journal of Zoology-Revue Canadienne De Zoologie*, 89**:** 892-899. DOI: 10.1139/z11-073

Mack, M. C., M. S. Bret-Harte, T. N. Hollingsworth, R. R. Jandt, E. A. G. Schuur, G. R. Shaver, and D. L. Verbyla. 2011. Carbon loss from an unprecedented Arctic tundra wildfire. *Nature*, 475**:** 489-492. DOI: 10.1038/nature10283

Mastepanov, M., C. Sigsgaard, M. Mastepanov, L. Ström, M. P. Tamstorf, M. Lund, and T. R. Christensen. 2013. Revisiting factors controlling methane emissions from high-Arctic tundra. *Biogeosciences*, 10**:** 5139-5158. DOI: 10.5194/bg-10-5139-2013

McGuire, A. D., L. G. Anderson, T. R. Christensen, S. Dallimore, L. D. Guo, D. J. Hayes, M. Heimann, T. D. Lorenson, et al. 2009. Sensitivity of the carbon cycle in the Arctic to climate change. *Ecological Monographs*, 79**:** 523-555. DOI: 10.1890/08-2025.1

McGuire, A. D., F. S. Chapin, J. E. Walsh, and C. Wirth. 2006. Integrated regional changes in arctic climate feedbacks: Implications for the global climate system. *Annual Review of Environment and Resources*, 31**:** 61-91. DOI: 10.1146/annurev.energy.31.020105.100253

McGuire, A. D., T. R. Christensen, D. Hayes, A. Heroult, E. Euskirchen, J. S. Kimball, C. Koven, P. Lafleur, et al. 2012. An assessment of the carbon balance of Arctic tundra: comparisons among observations, process models, and atmospheric inversions. *Biogeosciences*, 9**:** 3185-3204. DOI: 10.5194/bg-9-3185-2012

Melton, J. R., R. Wania, E. L. Hodson, B. Poulter, B. Ringeval, R. Spahni, T. Bohn, C. A. Avis, et al. 2013. Present state of global wetland extent and wetland methane modelling: conclusions from a model inter-comparison project (WETCHIMP). *Biogeosciences*, 10**:** 753-788. DOI: 10.5194/bg-10-753-2013

Miller, P. A., and B. Smith. 2012. Modelling Tundra Vegetation Response to Recent Arctic Warming. *Ambio*, 41**:** 281-291. DOI: 10.1007/s13280-012-0306-1

Monsi, M., and T. Saeki. 1953. On the factor light in plant communities and its importance for matter production. *Annals of Botany*, 95**:** 549-567. DOI: 10.1093/aob/mci052

Myers-Smith, I. H., B. C. Forbes, M. Wilmking, M. Hallinger, T. Lantz, D. Blok, K. D. Tape, M. Macias-Fauria, et al. 2011. Shrub expansion in tundra ecosystems: dynamics, impacts and research priorities. *Environmental Research Letters*, 6. DOI: 10.1088/1748-9326/6/4/045509

Olefeldt, D., M. R. Turetsky, P. M. Crill, and A. D. McGuire. 2013. Environmental and physical controls on northern terrestrial methane emissions across permafrost zones. *Global Change Biology*, 19**:** 589-603. DOI: 10.1111/gcb.12071

Olofsson, J., L. Oksanen, T. Callaghan, P. E. Hulme, T. Oksanen, and O. Suominen. 2009. Herbivores inhibit climate-driven shrub expansion on the tundra. *Global Change Biology,* 15**:** 2681-2693. DOI: 10.1111/j.1365-2486.2009.01935.x

Olofsson, J., S. Stark, and L. Oksanen. 2004. Reindeer influence on ecosystem processes in the tundra. *Oikos,* 105**:** 386-396. DOI: 10.1111/j.0030-1299.2004.13048.x

Pappas, C., S. Fatichi, S. Rimkus, P. Burlando, and M. O. Huber. 2015. The role of local-scale heterogeneities in terrestrial ecosystem modeling. *Journal of Geophysical Research-Biogeosciences,* 120**:** 341-360. DOI: 10.1002/2014jg002735

Pries, C. E. H., E. A. G. Schuur, and K. G. Crummer. 2012. Holocene Carbon Stocks and Carbon Accumulation Rates Altered in Soils Undergoing Permafrost Thaw. *Ecosystems,* 15**:** 162-173. DOI: 10.1007/s10021-011-9500-4

Reich, P. B., M. B. Walters, and D. S. Ellsworth. 1997. From tropics to tundra: Global convergence in plant functioning. *Proceedings of the National Academy of Sciences of the United States of America,* 94**:** 13730-13734. DOI: 10.1073/pnas.94.25.13730

Scheiter, S., L. Langan, and S. I. Higgins. 2013. Next-generation dynamic global vegetation models: learning from community ecology. *New Phytologist,* 198**:** 957-969. DOI: 10.1111/nph.12210

Schlesinger, W. H., and E. S. Bernhardt. 2013. *Biogeochemistry: An analysis of global change.* Waltham: Elsevier.

Schmidt, N. M., D. K. Kristensen, A. Michelsen, and C. Bay. 2012. High Arctic plant community responses to a decade of ambient warming. *Biodiversity (Ottawa),* 13**:** 191-199. DOI: 10.1080/14888386.2012.712093

Schuur, E. A. G., A. D. McGuire, C. Schadel, G. Grosse, J. W. Harden, D. J. Hayes, G. Hugelius, C. D. Koven, et al. 2015. Climate change and the permafrost carbon feedback. *Nature,* 520. DOI: 10.1038/nature14338

Serreze, M. C., and R. G. Barry. 2011. Processes and impacts of Arctic amplification: A research synthesis. *Global and Planetary Change,* 77**:** 85-96. DOI: 10.1016/j.gloplacha.2011.03.004

Sitch, S., B. Smith, I. C. Prentice, A. Arneth, A. Bondeau, W. Cramer, J. O. Kaplan, S. Levis, et al. 2003. Evaluation of ecosystem dynamics, plant geography and terrestrial carbon cycling in the LPJ dynamic global vegetation model. *Global Change Biology,* 9**:** 161-185. DOI: 10.1046/j.1365-2486.2003.00569.x

Sjoegersten, S., R. Llurba, A. Ribas, A. Yanez-Serrano, and M. T. Sebastia. 2012. Temperature and Moisture Controls of C Fluxes in Grazed Subalpine Grasslands. *Arctic Antarctic and Alpine Research,* 44**:** 239-246. DOI: 10.1657/1938-4246-44.2.239

Sjogersten, S., R. van der Wal, M. Loonen, and S. J. Woodin. 2011. Recovery of ecosystem carbon fluxes and storage from herbivory. *Biogeochemistry,* 106**:** 357-370. DOI: 10.1007/s10533-010-9516-4

Smith, B., I. C. Prentice, and M. T. Sykes. 2001. Representation of vegetation dynamics in the modelling of terrestrial ecosystems: comparing two contrasting approaches within European climate space. *Global Ecology and Biogeography,* 10**:** 621-637. DOI: 10.1046/j.1466-822X.2001.t01-1-00256.x

Smith, B., D. Warlind, A. Arneth, T. Hickler, P. Leadley, J. Siltberg, and S. Zaehle. 2014. Implications of incorporating N cycling and N limitations on primary production in an individual-based dynamic vegetation model. *Biogeosciences,* 11**:** 2027-2054. DOI: 10.5194/bg-11-2027-2014

Smith, J., and P. Smith. 2007. *Introduction to Environmental Modelling*. Oxford: Oxford University Press.

Stams, A. J. M., and C. M. Plugge. 2010. The microbiology of methanogenesis. In *Methane and climate change,* eds. D. Reay, P. Smith, and A. Van Amstel, 14-27 pp. London: Earthscan.

Stark, S., and H. Ylänne. 2015. Grazing in Arctic peatlands - an unknown agent in the global carbon budget. *Environmental Research Letters,* 10.

Ström, L., and T. R. Christensen. 2007. Below ground carbon turnover and greenhouse gas exchanges in a sub-arctic wetland. *Soil Biology & Biochemistry,* 39**:** 1689-1698. DOI: 10.1016/j.soilbio.2007.01.019

Ström, L., A. Ekberg, M. Mastepanov, and T. R. Christensen. 2003. The effect of vascular plants on carbon turnover and methane emissions from a tundra wetland. *Global Change Biology,* 9**:** 1185-1192. DOI: 10.1046/j.1365-2486.2003.00655.x

Ström, L., J. M. Falk, K. Skov, M. Jackowicz-Korczynski, M. Mastepanov, T. R. Christensen, M. Lund, and N. M. Schmidt. 2015. Controls of spatial and temporal variability in CH 4 flux in a high arctic fen over three years *Biogeochemistry (accepted)*.

Ström, L., T. Tagesson, M. Mastepanov, and T. R. Christensen. 2012. Presence of Eriophorum scheuchzeri enhances substrate availability and methane emission in an Arctic wetland. *Soil Biology & Biochemistry,* 45**:** 61-70. DOI: 10.1016/j.soilbio.2011.09.005

Tang, J., P. A. Miller, P. Crill, S. Olin, and P. Pilesjö. 2014b. Investigating the influence of two different flow routing algorithms on soil – water – vegetation interactions using the dynamic ecosystem model LPJ-GUESS. *Ecohydrology*. DOI: 10.1002/eco.1526

Tang, J., P. Pilesjo, P. A. Miller, A. Persson, Z. L. Yang, E. Hanna, and T. V. Callaghan. 2014a. Incorporating topographic indices into dynamic ecosystem modelling using LPJ-GUESS. *Ecohydrology,* 7**:** 1147-1162. DOI: 10.1002/eco.1446

Tarnocai, C., J. G. Canadell, E. A. G. Schuur, P. Kuhry, G. Mazhitova, and S. Zimov. 2009. Soil organic carbon pools in the northern circumpolar permafrost region. *Global Biogeochemical Cycles,* 23. DOI: 10.1029/2008gb003327

Turetsky, M. R., B. Bond-Lamberty, E. Euskirchen, J. Talbot, S. Frolking, A. D. McGuire, and E. S. Tuittila. 2012. The resilience and functional role of moss in boreal and arctic ecosystems. *New Phytologist,* 196**:** 49-67. DOI: 10.1111/j.1469-8137.2012.04254.x

Verheijen, L. M., V. Brovkin, R. Aerts, G. Bonisch, J. H. C. Cornelissen, J. Kattge, P. B. Reich, I. J. Wright, et al. 2013. Impacts of trait variation through observed trait-climate relationships on performance of an Earth system model: a conceptual analysis. *Biogeosciences,* 10**:** 5497-5515. DOI: 10.5194/bg-10-5497-2013

Wania, R., J. R. Melton, E. L. Hodson, B. Poulter, B. Ringeval, R. Spahni, T. Bohn, C. A. Avis, et al. 2013. Present state of global wetland extent and wetland methane modelling: methodology of a model inter-comparison project (WETCHIMP). *Geoscientific Model Development,* 6**:** 617-641. DOI: 10.5194/gmd-6-617-2013

Wania, R., I. Ross, and I. C. Prentice. 2009a. Integrating peatlands and permafrost into a dynamic global vegetation model: 1. Evaluation and sensitivity of physical land surface processes. *Global Biogeochemical Cycles,* 23. DOI: 10.1029/2008gb003412

Wania, R., I. Ross, and I. C. Prentice. 2009b. Integrating peatlands and permafrost into a dynamic global vegetation model: 2. Evaluation and sensitivity of vegetation and carbon cycle processes. *Global Biogeochemical Cycles,* 23. DOI: 10.1029/2008gb003413

Wania, R., I. Ross, and I. C. Prentice. 2010. Implementation and evaluation of a new methane model within a dynamic global vegetation model: LPJ-WHyMe v1.3.1. *Geoscientific Model Development,* 3**:** 565-584. DOI: 10.5194/gmd-3-565-2010

Woo, M. K., and K. L. Young. 2003. Hydrogeomorphology of patchy wetlands in the High Arctic, polar desert environment. *Wetlands,* 23**:** 291-309. DOI: 10.1672/8-20

Wullschleger, S. D., H. E. Epstein, E. O. Box, E. S. Euskirchen, S. Goswami, C. M. Iversen, J. Kattge, R. J. Norby, et al. 2014. Plant functional types in Earth system models: past experiences and future directions for application of dynamic vegetation models in high-latitude ecosystems. *Annals of Botany,* 114**:** 1-16. DOI: 10.1093/aob/mcu077

Xu, L., R. B. Myneni, F. S. Chapin, T. V. Callaghan, J. E. Pinzon, C. J. Tucker, Z. Zhu, J. Bi, et al. 2013. Temperature and vegetation seasonality diminishment over northern lands. *Nature Climate Change,* 3**:** 581-586. DOI: 10.1038/nclimate1836

Yu, Q., H. Epstein, and D. Walker. 2009. Simulating the effects of soil organic nitrogen and grazing on arctic tundra vegetation dynamics on the Yamal Peninsula, Russia. *Environmental Research Letters,* 4. DOI: 10.1088/1748-9326/4/4/045027

Yu, Q., H. E. Epstein, D. A. Walker, G. V. Frost, and B. C. Forbes. 2011. Modeling dynamics of tundra plant communities on the Yamal Peninsula, Russia, in response to climate change and grazing pressure. *Environmental Research Letters,* 6. DOI: 10.1088/1748-9326/6/4/045505

Zhang, W., P. A. Miller, B. Smith, R. Wania, T. Koenigk, and R. Doscher. 2013. Tundra shrubification and tree-line advance amplify arctic climate warming: results from an individual-based dynamic vegetation model. *Environmental Research Letters,* 8. DOI: 10.1088/1748-9326/8/3/034023

Institutionen för naturgeografi och ekosystemvetenskap, Lunds Universitet.

Student examensarbete (Seminarieuppsatser). Uppsatserna finns tillgängliga på institutionens geobibliotek, Sölvegatan 12, 223 62 LUND. Serien startade 1985. Hela listan och själva uppsatserna är även tillgängliga på LUP student papers (https://lup.lub.lu.se/student-papers/search/) och via Geobiblioteket (www.geobib.lu.se)

The student thesis reports are available at the Geo-Library, Department of Physical Geography and Ecosystem Science, University of Lund, Sölvegatan 12, S-223 62 Lund, Sweden. Report series started 1985. The complete list and electronic versions are also electronic available at the LUP student papers (https://lup.lub.lu.se/student-papers/search/) and through the Geo-library (www.geobib.lu.se)

335 Fei Lu (2015) Compute a Crowdedness Index on Historical GIS Data- A Case Study of Hög Parish, Sweden, 1812-1920

336 Lina Allesson (2015) Impact of photo-chemical processing of dissolved organic carbon on the bacterial respiratory quotient in aquatic ecosystems

337 Andreas Kiik (2015) Cartographic design of thematic polygons: a comparison using eye-movement metrics analysis

338 Iain Lednor (2015) Testing the robustness of the Plant Phenology Index to changes in temperature

339 Louise Bradshaw (2015) Submerged Landscapes - Locating Mesolithic settlements in Blekinge, Sweden

340 Elisabeth Maria Farrington (2015) The water crisis in Gaborone: Investigating the underlying factors resulting in the 'failure' of the Gaborone Dam, Botswana

341 Annie Forssblad (2015) Utvärdering av miljöersättning för odlingslandskapets värdefulla träd

342 Iris Behrens, Linn Gardell (2015) Water quality in Apac-, Mbale- & Lira district, Uganda - A field study evaluating problems and suitable solutions

343 Linnéa Larsson (2015) Analys av framtida översvämningsrisker i Malmö - En fallstudie av Castellums fastigheter

344 Ida Pettersson (2015) Comparing Ips Typographus and Dendroctonus ponderosas response to climate change with the use of phenology models

345 Frida Ulfves (2015) Classifying and Localizing Areas of Forest at Risk of Storm Damage in Kronoberg County

346 Alexander Nordström (2015) Förslag på dammar och skyddsområde med hjälp av GIS: En studie om löv- och klockgroda i Ystad kommun, Skåne

347 Samanah Seyedi-Shandiz (2015) Automatic Creation of Schematic Maps - A Case Study of the Railway Network at the Swedish Transport Administration

348 Johanna Andersson (2015) Heat Waves and their Impacts on Outdoor Workers – A Case Study in Northern and Eastern Uganda

349 Jimmie Carpman (2015) Spatially varying parameters in observed new particle formation events

350 Mihaela – Mariana Tudoran (2015) Occurrences of insect outbreaks in Sweden in relation to climatic parameters since 1850

351 Maria Gatzouras (2015) Assessment of trampling impact in Icelandic natural areas in experimental plots with focus on image analysis of digital photographs

352 Gustav Wallner (2015) Estimating and evaluating GPP in the Sahel using

MSG/SEVIRI and MODIS satellite data

353 Luisa Teixeira (2015) Exploring the relationships between biodiversity and benthic habitat in the Primeiras and Segundas Protected Area, Mozambique

354 Iris Behrens & Linn Gardell (2015) Water quality in Apac-, Mbale- & Lira district, Uganda - A field study evaluating problems and suitable solutions

355 Viktoria Björklund (2015) Water quality in rivers affected by urbanization: A Case Study in Minas Gerais, Brazil

356 Tara Mellquist (2015) Hållbar dagvattenhantering i Stockholms stad - En riskhanteringsanalys med avseende på långsiktig hållbarhet av Stockholms stads dagvattenhantering i urban miljö

357 Jenny Hansson (2015) Trafikrelaterade luftföroreningar vid förskolor – En studie om kvävedioxidhalter vid förskolor i Malmö

358 Laura Reinelt (2015) Modelling vegetation dynamics and carbon fluxes in a high Arctic mire

359 Emelie Linnéa Graham (2015) Atmospheric reactivity of cyclic ethers of relevance to biofuel combustion

360 Filippo Gualla (2015) Sun position and PV panels: a model to determine the best orientation

361 Joakim Lindberg (2015) Locating potential flood areas in an urban environment using remote sensing and GIS, case study Lund, Sweden

362 Georgios-Konstantinos Lagkas (2015) Analysis of NDVI variation and snowmelt around Zackenberg station, Greenland with comparison of ground data and remote sensing.

363 Carlos Arellano (2015) Production and Biodegradability of Dissolved Organic Carbon from Different Litter Sources